C.P. No. 1006

C.P. No. 1006

MINISTRY OF TECHNOLOGY

AERONAUTICAL RESEARCH COUNCIL

CURRENT PAPERS

The Longitudinal Characteristics of Three Slender 'Mild Ogee' Wings at Mach Numbers from 0.4 to 2.0

by

D. G. Mabey, M.Sc. and G. P. Ilott, B.Sc.

LONDON: HER MAJESTY'S STATIONERY OFFICE

1968

PRICE 15s 6d NET

U.D.C. 533.693.3 : 533.6.011.3 : 533.6.013.13 : 533.6.013.152
533.6.013.12 : 533.6.071

C.P. No. 1006*
August 1967

THE LONGITUDINAL CHARACTERISTICS OF THREE SLENDER "MILD OGEE" WINGS AT MACH NUMBERS FROM 0.4 TO 2.0

by

D.G. Mabey, M.Sc. (Eng)

G.P. Ilott, B.Sc.

SUMMARY

Wind tunnel measurements of lift, pitching moment and drag on one plane and two cambered wings of "mild ogee" planform ($p = 8/15$) are reported. These measurements are supplemented by vapour screen and oil flow observations.

The wings were designed by slender wing theory for attached flow along the leading-edge at particular values of lift and pitching moment. The design and measured attachment conditions agreed fairly well. The non-linear lift developed could be related with the type of vortex development above the attachment incidence.

* Replaces R.A.E. Tech. Report 67202 - A.R.C. ~~1006~~ 30166

CONTENTS

1 INTRODUCTION

To assist the design of slender wings for flight at supersonic speeds three "mild ogee" wings were tested in the 3 × 3ft wind tunnel over the Mach number range from M = 0.40 to 2.00 in January 1961. These wings had a common planform, with a value of planform parameter p = 0.533 intermediate between the high value of wings tested by Squire[1,2,3] and the low value of wings tested by Courtney[4] and Taylor[5]. The tests were intended to provide more data on the effects of p on camber design and lift dependent drag.

This paper compares the measured and calculated forces and moments on the wings and describes the types of flow observed at off-design conditions.

2 EXPERIMENTAL DETAILS

2.1 Model design

The three wings had a common planform (Fig.1 and Table 1); as they followed the eight wings discussed in Refs.1, 2 and 3 they were designated wings 9, 10 and 11.

Wing 9 was uncambered. The cambered wings were designed by slender wing theory for attached flow at the leading-edge with a given load distribution. The method of camber design was outlined by Weber[6]. For both wings the spanwise camber was restricted to a region outboard of a "shoulder position" defined by $y = (0.5 + 0.25x)\ (Sx)$. Wing 10 was designed for flow attachment at a lift coefficient of 0.05 with the centre of pressure at $0.547\ c_o$. This was $0.07\ c_o$ forward of the slender wing aerodynamic centre position, $0.617\ c_o$. The pitching moment increment ΔC_m was thus 0.0035 on c_o (or 0.0053 on $\bar{\bar{c}}$). The design of this wing was discussed in Ref.7 and details of the design loading and the camber shapes are given in Figs.2 and 3 and Table 1. Wing 11 was designed for the same pitching moment increment as wing 10 ($\Delta C_m = 0.0053$ on $\bar{\bar{c}}$) at zero lift coefficient. The design load distribution for Wing 11 was that of Wing 10 less the slender wing load distribution on an uncambered wing with $C_L = 0.05$. Details of Wing 11* are given in Figs.2 and 3 of Table 1.

The thickness was added to the camber surface as on earlier wings of this series[1,2,3]. The diamond shaped thickness distribution was added to the

---

*Although the centre line camber, C(X), for Wing 10 was determined algebraically, C(X) for wing 11 was found numerically.

camber surfaces so that areas of spanwise stations were the same for all three wings. Typical cross-sections are shown in Fig.2.

A small body was added to the rear of the model to shield the balance and sting support. On the cambered models this shield was not quite symmetric, however, the estimated errors caused by this asymmetry on the wing pitching moment are small.

Wing 9 was made completely of steel but Wings 10 and 11 were made of glass-cloth and araldite on a steel core. The models were given a matt black paint finish to facilitate flow visualization.

2.2 Test range

The tests were made in the transonic and supersonic sections of the 3 × 3ft tunnel at R.A.E. Bedford. The lift, pitching moment and drag were measured in the nominal incidence* range -2° to $+13^\circ$ (one degree steps) at Mach numbers of 0.40, 0.70, 0.85, 0.90, 0.94, 0.98, 1.02, 1.42, 1.61, 1.82 and 2.00. In addition, surface oil flow and vapour screen patterns were obtained at selected conditions where changes in types of flow were expected.

The test Reynolds number was 1.6×10^6 per foot, except at $M = 2.0$ when it was reduced to 1.35×10^6 per foot because of a tunnel power limitation.

In all force tests bands of distributed roughness were applied to fix transition of the boundary layer on both surfaces of the wing. The roughness bands consisted of a mixture of carborundum grains and thin aluminium paint applied so that closely spaced individual grains projected from a paint base about 0.001 inch thick. The height of the particles was 0.003 inch at speeds up to 1.02 and 0.007 inch at higher speeds. The roughness bands were half an inch wide (normal to the leading-edge) and started an eighth of an inch inboard of the edge.

This roughness distribution did fix transition on other wings of this series[3] except possibly at $M = 1.02$ and 2.00 for a small incidence range. However, the drag results on Wing 9 at $M = 1.8$ and 2.0 revealed a "bucket" of the type previously associated[8] with laminar flow as shown in Fig.4. An investigation of the boundary layer state using azobenzene did, in fact, reveal large areas of laminar flow (Fig.5). The minimum height of roughness

*Incidence for the cambered wings is defined as the incidence of the plane containing the wing apex and the centre section of the wing trailing-edge.

needed to fix transition at the comparatively low Reynolds numbers then available in the 3ft tunnel was subsequently determined and was reported in Ref.9. This investigation included drag measurements on Wing 9 with different roughness distributions over a wide range of Reynolds number but for consistency with wings 10 and 11, only data with roughness particles 0.007 inch high were quoted here.

2.3 Accuracy

The balance results have been corrected for interaction effects and sting deflection before being reduced to coefficient forms; for all wings these coefficients are based on the dimensions of the common planform. Moments (based on $\bar{\bar{c}}$) are referred to the 48.5% point of the aerodynamic mean chord (66% of the root chord) so that the change of aerodynamic centre position with Mach number is emphasised (Figs.10-12). The drag has been corrected to a base pressure equal to free stream static pressure. No corrections have been applied to the measured pitching moment or drag for the small distortion caused by the sting shield.

The incidence and pitching moment have been corrected for flow deflection and curvature in the tunnel stream. The flow corrections were found for the uncambered wing and the same corrections applied to all the cambered wings: the maximum corrections were $\Delta\alpha = 0.2^\circ$ and $\Delta C_m = 0.0010$. Previous tests in this series[3] have justified this procedure.

No corrections have been applied for tunnel interference; this interference is, of course, absent at supersonic speeds when the bow shock wave is reflected clear of the model ($M > 1.3$). There is, however, some interference at subsonic and transonic speeds. Previous tests have shown that these effects are small except near $M = 1.00$. Here the Mach number error may be as large as 0.02; the free stream Mach number being less than the quoted tunnel Mach number.

Apart from this tunnel interference it is estimated that the accuracy of the results is as follows

C_L	± 0.003
C_m	± 0.0006
C_D	± 0.0004 at $C_L = 0$ ± 0.0010 at $C_L = 0.3$
α	$\pm 0.05^\circ$

3 RESULTS

3.1 Lift and pitching moment

The variation of lift coefficient with incidence is plotted in Figs.6-8 for Wings 9-11. Appreciable non-linear lift is developed from flow separations at the sharp leading-edges, particularly at subsonic speeds. The cambered wings should have attached flow along the leading-edge at the design condition, which may be compared with the incidence ($\bar{\alpha}$) for minimum lift curve slope near M = 1.0 (the Mach number appropriate to the slender wing design value $\beta S_T/c_o = 0$). Fair agreement is shown in the following table.

Comparison of attachment conditions near M = 1.0

Wing	Measured		Design	
	$\bar{\alpha}$	$\bar{C}_L$	$\bar{\alpha}$	$\bar{C}_L$
10	4.0°	0.075	3.2°	0.05
11	1.0°	0.012	0.8°	0

The lift development for the three wings above the attachment incidence may be compared[3] by plotting $C_L - \bar{C}_L$ against $\alpha - \bar{\alpha}$, Fig.9. The lift on Wings 9 and 11 correlates exactly but much more non-linear lift is developed by Wing 10. This is discussed in 3.3 below.

Near the attachment incidence the slopes of the curves do not vary significantly with Mach number and correspond fairly well with the slender wing value appropriate to M = 1.0 ($dC_L/d\alpha = \pi A/2$), (Fig.9b).

Above the attachment incidence non-linear lift develops; this is considerable at M = 0.40 (Fig.9a), reaches a maximum near M = 1.0 but decreases as the Mach number increases to M = 2.0 (Fig.9b). The non-linear lift measured on Wings 9 and 11 at M = 1.02 compares favourably with that given by Mangler and Smith[10,11].

The variation of pitching moment coefficient C_m with lift coefficient for Wings 9-11 is shown in Figs.10-12. The curves are fairly smooth and clearly show the rearward movement of aerodynamic centre, as the Mach number increases from subsonic to supersonic speeds. The aerodynamic centre positions on the root chord c_o are given at lift coefficients of 0.05, 0.10, and 0.20 in Fig.13 and the corresponding centre of pressure positions are given in Fig.14.

It is difficult to assess the success of the camber designs of Wings 10 and 11 as the slender wing theory strictly applies only at M = 1.0. At this Mach number tunnel interference effects are critical. A small error in Mach number can mean large errors in the shock wave positions on both wing surfaces - and hence large errors in lift and pitching moment. However, the measured centre of pressure positions on Wing 10 at supersonic speeds, when extrapolated to M = 1.0, correspond quite well with the measured value at M = 0.98 and with the design position (Fig.14, C_L = 0.05). Since Wing 11 was designed for C_L = 0 a comparison of the measured and design values of zero lift pitching moment, C_{m_o}, is given in Fig.15. The measured C_{m_o} at M = 1.00 (0.0030) does not agree with the design value (0.0053). However the corresponding curve for Wing 10 indicates that C_{m_o} increases rapidly with M near M = 1.00 so that the apparent discrepancy could be attributed to interference effects. It is interesting to note that Wing 11 does achieve a C_{m_o} = 0.055 at M = 1.42.

The general success of both the camber designs is indicated by the plot of trimmed C_L against Mach number in Fig.16: a trimmed C_L of about 0.05 is obtained on both wings at M = 2.0. In deriving these curves, a centre of gravity position of 0.41 $\bar{\bar{c}}$ (0.61 c_o) was chosen, corresponding to the most forward position of the aerodynamic centre at likely flight conditions at low Mach number (see Fig.14).

3.2 Drag

The variation of drag coefficient with lift coefficient for Wings 9-11 is given in Figs.17-19. These curves approximate to parabolae except when the roughness is ineffective and there is a "laminar bucket" near zero lift. On this planform at supersonic speeds it appears easier to fix transition on the more highly cambered surfaces, e.g. Wing 10, the wing with most camber has no laminar bucket in the test range, Wing 11 has a laminar bucket at M = 2.0 and wing 9 at 1.8 and 2.0. The reason for this effect of leading-edge camber on transition is uncertain but it has been observed previously[12] at $M = 2.0$ on some highly swept arrow wings with sharp leading-edges. Fig.5 of Ref.12 is particularly relevant to the present tests. Carborundum slightly higher than 0.007 inch was used and the Reynolds number range extended from $R = 0.5 \times 10^6$ to 4.4×10^6. Transition was always fixed on the cambered wing but on the plane wing transition occurred from $R = 1.3 \times 10^6$ to 2.0×10^6 (c.f. the present test Reynolds number 1.35×10^6 with particles only 0.007 inch high).

The measured variation with Mach number of C_{D_o} for Wing 9 is plotted in Fig.20. The estimated total drag (the wave drag of the model including the fairing plus skin friction) is also plotted. At subsonic and transonic speeds the measured drag is 10% higher than the estimated skin friction as in previous tests with a model having the same area distribution[3]: this difference may be caused by sting interference or it could be form drag. At supersonic speeds there is excellent agreement between the measured and estimated drags at $M = 1.42$ and 1.61, the measured C_{D_o} being 0.0002 lower than the estimate. However, at 1.82 and 2.00 the measured C_{D_o} is lower than the estimate due to the failure to fix transition of the boundary layer. It was assumed in the analysis of the drag due to lift that the plane wing C_{D_o} with fixed transition at $M = 1.82$ and 2.00, C'_{D_o}, is also 0.0002 lower than the estimate. [If the axial force for $M = 1.82$ and 2.00 is plotted against $|\alpha|$ and the laminar bucket faired out the value of axial force at $\alpha = 0$, (C_{D_o}), is in fact about 0.0002 below the estimate for both Mach numbers.]

Fig.21 shows the variation of the drag due to lift factor with lift coefficient and Mach number for the three wings. C_D is the measured drag coefficient on the respective wings (with roughness particles 0.007 inch high).

The variation of the drag due to lift factors with slenderness parameter $\beta S_T/c_o$ at C_L's of 0.10 and 0.20 from Fig.21 are plotted in Fig.22. Wings 9 and 11 are nearly identical and lie above Courtney's correlation curve[13]. In contrast Wing 10 lies close to Courtney's curve, although still above the design value[7] at $\beta S_T/c_o = 0.374$. This improvement in the drag due to lift contributes to the favourable lift-to-drag ratios measured on Wing 10 compared to Wings 9 and 11; the wing lift-to-drag ratios are presented in Fig.23.

3.3 Vortex development

The non-linear lift developed on Wings 9 and 11 above the attachment incidence is nearly the same. In contrast Wing 10 develops considerably more non-linear lift than Wings 9 and 11 when $\alpha - \bar{\alpha}$ is greater than about 3°. These results can be related with the vortex development observed on the wings.

The first useful clue to the vortex development was observed on the tunnel schlieren at $M = 2.0$ with carborundum 0.020 inch high on the wings (during the roughness investigation reported in Ref.9). The shock waves from the particles were then clearly visible along the leading-edge (c.f. 3.2 above) at the attachment incidence. When the incidence increased these shock waves disappeared as the roughness became immersed in the separated flow from the leading-edge. For Wings 9 and 11 measurements revealed that the region without shock waves increased gradually as incidence increased (Fig.24). For Wing 10, however, the shock waves seemed to disappear suddenly between $\alpha = 7^{\circ}$ to 8° ($\alpha - \bar{\alpha}$ between 3° and 4°) and it was impossible to measure this movement.

Observation* of the vortices using the vapour screen technique[14] confirmed the close similarity of the flow on Wings 9 and 11 (Figs.25a and 25c). On Wings 9 and 11 the leading-edge vortex develops approximately conically as incidence increases. On Wing 10, in addition to the leading-edge vortex an array of streamwise vortices seems to develop as incidence increases (Fig.25b). Between $\alpha = 7.3^{\circ}$ and 8.3° the leading-edge vortex and the streamwise vortices suddenly coalesce≠. The vortex on Wing 10 is then wider than on Wings 9 and 11 (c.f. Fig.25a, $\alpha - \bar{\alpha} = 4.1^{\circ}$ and Fig.25b, $\alpha - \bar{\alpha} = 4.2^{\circ}$). This wider spanwise extent of the vortex on wing 10 probably produces the larger non-linear lift (c.f. Fig.9, Wings 10 and 9). The vapour screen on Wing 10 at $M = 1.4$ with and without roughness was identical with that at $M = 1.8$ so that the boundary layer state could not be determining the vortex development.

---

*In these experiments a television camera mounted on the model sting recorded the vapour screen. Photographs of the television pictures for one station on the wing are reproduced in Fig.25.

≠It is possible that this "array" is really an array of subsidiary vortex cores along the main vortex sheet and thus a three-dimensional counterpart to similar arrays observed by Pierce[15] on two-dimensional plates moved in still air. The present investigation could not go far enough to establish the nature of the vortex development in sufficient detail.

The oil flow photographs now presented illustrate additional details of the vortex development on Wings 9 and 10. Fig.26 shows some typical oil flow photographs taken on Wing 9. Fig.26a, at $M = 2.0$ and $\alpha = 5.1^{\circ}$ shows a similar flow to that on a slender delta wing. The vortex development is nearly conical and is characterised by a strong primary vortex and a secondary separation near the leading edge; the roughness was removed to show this secondary separation. Fig.26b at $M = 0.40$, $\alpha = 5.1^{\circ}$ is included to recall that if wings are sufficiently slender there is close similarity between the separated flows at subsonic and supersonic speeds although the non-linear lift is larger at subsonic speeds. The vortex is roughly elliptical in section on the vapour screen at supersonic speeds (Fig.25a) and is known to be roughly circular in section at subsonic speeds. The change in width of the vortex can be seen in Fig.26. Here the intersection of the attachment line and the trailing-edge moves outboard from $0.64\ S_T$ at $M = 2.0$ to $0.77\ S_T$ at $M = 0.40$.

Fig.27 shows some typical oil flow photographs taken on Wing 10 at $M = 1.4$ without roughness. The flow at 7.3° shows a complex array of streamwise vortices covering most of the planform (Fig.27a). A similar array of vortices has been observed previously on delta wings and attributed[16] to the rolling up of the boundary layer vorticity under the influence of the spanwise pressure gradient. The flow at 8.3° apparently shows only one large vortex but a careful examination reveals a few streamwise vortices inboard of the main vortex (Fig.27b).

4 CONCLUSIONS

Tests of three mild ogee wings in the 3ft tunnel at subsonic and supersonic speeds showed that a prescribed type of lift and centre of pressure position[6,7] was achieved on both cambered wings.

The vortex development on Wings 9 and 11 was approximately conical and similar to that on a slender delta. The vortex development on Wing 10 at supersonic speeds was characterised initially by what seems to be an array of small streamwise vortices in addition to the leading-edge vortex. The streamwise vortices coalesced suddenly with the leading-edge vortex as incidence was increased. This single vortex extended spanwise further than the vortex on Wings 9 and 11 at comparable incidences; the increase in size probably accounted for the larger non-linear lift increment of Wing 10.

TABLE 1

GEOMETRY OF WINGS 9-11

Root chord	c_o	$=$ 22 inches
Aerodynamic mean chord	$\bar{\bar{c}}$	$= 37/56 \cdot c_o = 14.545$ inches
Wing area	S	$= 16/15 \cdot S_T\, c_o = 129.1$ square inches
Aspect ratio	A	$= 0.9375$
Equation of leading edge	y	$= S_T\, x(1 + x^3 - x^4)$
Planform parameter	p	$= 8/15 = 0.533$
Slenderness factor	S_T/c_o	$= 0.25$
Newby area distribution	$A(x)$	$= 12V\, c_o^2\, x^2(1 - x)$
where	V	$=$ volume$/c_o^3$
For Wings 9-11	V	$= 0.00584$.

Hence non dimensional volume factor

$$\tau = \text{wing volume/wing area}^{3/2} = 0.0424 \; .$$

Wing 10 Equation of centre line camber

$$z = 0.0395[1.413 - (x + 2.648x^2 - 3.644x^3 + 1.409x^4)] \; .$$

Wing 11 - Table of centre line camber

x	z
0.0	0.0136
0.1	0.0129
0.2	0.0112
0.3	0.0088
0.4	0.0063
0.5	0.0039
0.6	0.0021
0.7	0.0013
0.8	0.0002
0.9	0.0000
1.0	0.0000

TABLE 2

RESULTS - WING 9

M	α	C_L	C_m	C_D
0.40	-2.04	-0.051	-0.0032	0.0098
	-1.07	-0.026	-0.0019	0.0090
	0	-0.001	0	0.0090
	+1.02	+0.024	+0.0021	0.0093
	1.99	0.048	0.0036	0.0105
	3.06	0.079	0.0054	0.0130
	4.09	0.108	0.0077	0.0163
	5.11	0.141	0.0095	0.0212
	6.14	0.178	0.0106	0.0271
	7.17	0.215	0.0139	0.0346
	8.20	0.256	0.0171	0.0440
	9.23	0.296	0.0199	0.0549
	10.27	0.336	0.0231	0.0676
	11.30	0.378	0.0264	0.0816
	12.34	0.423	0.0301	0.0983
0.70	-2.06	-0.051	-0.0032	0.0099
	-1.08	-0.027	-0.0017	0.0091
	0	-0.002	0	0.0088
	+1.03	0.021	0.0018	0.0097
	2.02	0.050	0.0032	0.0106
	3.10	0.079	0.0047	0.0134
	4.14	0.113	0.0064	0.0168
	5.18	0.149	0.0082	0.0218
	6.23	0.186	0.0100	0.0279
	7.27	0.223	0.0121	0.0354
	8.32	0.266	0.0145	0.0457
	9.37	0.307	0.0170	0.0571
	10.43	0.349	0.0192	0.0702
	11.48	0.396	0.0221	0.0863
	12.54	0.440	0.0250	0.1032
0.85	-2.02	-0.054	-0.0033	0.0097
	-1.09	-0.028	-0.0017	0.0093
	0	-0.001	0	0.0086
	1.04	+0.023	0.0015	0.0094
	2.03	0.052	0.0025	0.0104
	3.12	0.085	0.0039	0.0132
	4.17	0.121	0.0053	0.0171
	5.22	0.158	0.0066	0.0225
	6.28	0.197	0.0083	0.0293
	7.33	0.238	0.0093	0.0379
	8.39	0.281	0.0112	0.0482
	9.45	0.327	0.0124	0.0609
	10.51	0.370	0.0143	0.0748
	11.58	0.418	0.0158	0.0917
	12.64	0.465	0.0175	0.1103

(Contd.)

TABLE 2 (Contd.)

M	α	C_L	C_m	C_D
0.90	-2.02	-0.060	-0.0025	0.0098
	-1.03	-0.028	-0.0014	0.0091
	0	-0.003	0	0.0084
	1.04	0.024	0.0012	0.0091
	2.03	0.054	0.0028	0.0109
	3.12	0.086	0.0036	0.0136
	4.17	0.122	0.0050	0.0172
	5.21	0.158	0.0060	0.0225
	6.26	0.199	0.0071	0.0296
	7.32	0.241	0.0081	0.0385
	8.37	0.284	0.0093	0.0490
	9.43	0.331	0.0102	0.0617
	10.48	0.374	0.0116	0.0758
	11.54	0.421	0.0130	0.0926
	12.60	0.469	0.0140	0.1113
0.94	-2.02	-0.056	-0.0029	0.0098
	-1.08	-0.029	-0.0017	0.0090
	0	-0.003	0	0.0086
	1.04	0.024	0.0015	0.0092
	2.04	0.055	0.0027	0.0108
	3.13	0.088	0.0036	0.0134
	4.18	0.125	0.0047	0.0175
	5.22	0.162	0.0053	0.0228
	6.27	0.204	0.0062	0.0302
	7.32	0.245	0.0071	0.0390
	8.38	0.290	0.0079	0.0499
	9.43	0.339	0.0080	0.0635
	10.49	0.383	0.0086	0.0782
	11.55	0.431	0.0094	0.0951
	12.60	0.478	0.0100	0.1142
0.98	-2.02	-0.059	-0.0023	0.0104
	-1.03	-0.029	-0.0016	0.0093
	+0.01	-0.003	0	0.0087
	1.05	0.025	0.0015	0.0095
	2.04	0.055	0.0021	0.0115
	3.13	0.091	0.0027	0.0144
	4.18	0.129	0.0031	0.0187
	5.22	0.167	0.0036	0.0245
	6.32	0.211	0.0037	0.0314
	7.32	0.257	0.0031	0.0414
	8.37	0.300	0.0031	0.0524
	9.42	0.351	0.0022	0.0665
	10.47	0.397	0.0018	0.0819
	11.51	0.445	0.0001	0.0993
	12.56	0.497	-0.0011	0.1195

(Contd.)

TABLE 2 (Contd.)

M	α	C_L	C_m	C_D
1.02	-2.06	-0.058	-0.0002	0.0125
	-1.03	-0.029	-0.0011	0.0117
	0	-0.005	0	0.0111
	1.04	0.024	+0.0010	0.0115
	2.03	0.060	0.0007	0.0138
	3.12	0.097	0.0004	0.0166
	4.16	0.134	0	0.0210
	5.20	0.177	-0.0011	0.0268
	6.25	0.222	-0.0016	0.0351
	7.29	0.262	-0.0022	0.0442
	8.34	0.308	-0.0031	0.0558
	9.38	0.354	-0.0040	0.0692
	10.44	0.403	-0.0044	0.0851
	11.49	0.450	-0.0055	0.1025
	12.54	0.494	-0.0058	0.1211
1.42	-1.96	-0.052	+0.0007	+0.0127
	-0.93	-0.023	+0.0004	+0.0117
	+0.10	+0.006	-0.0003	+0.0114
	+1.14	+0.033	-0.0007	+0.0122
	+2.17	+0.062	-0.0013	+0.0136
	+3.20	+0.093	-0.0021	+0.0160
	+4.24	+0.128	-0.0029	+0.0201
	+5.28	+0.163	-0.0038	+0.0254
	+6.32	+0.199	-0.0046	+0.0322
	+7.36	+0.235	-0.0052	+0.0402
	+8.40	+0.272	-0.0059	+0.0499
	+9.45	+0.308	-0.0064	+0.0607
	+10.49	+0.345	-0.0069	+0.0733
	+11.54	+0.381	-0.0073	+0.0873
	+12.58	+0.418	-0.0076	+0.1026
	+0.09	-0.008	+0.0002	+0.0113
1.61	-1.86	-0.044	+0.0002	+0.0119
	-0.83	-0.018	0	+0.0111
	+0.19	+0.001	0	+0.0106
	+1.23	+0.033	-0.0007	+0.0115
	+2.26	+0.064	-0.0014	+0.0131
	+3.20	+0.093	-0.0021	+0.0156
	+4.23	+0.126	-0.0028	+0.0193
	+5.27	+0.158	-0.0035	+0.0243
	+6.41	+0.191	-0.0041	+0.0306
	+7.45	+0.224	-0.0047	+0.0381
	+8.49	+0.257	-0.0051	+0.0472
	+9.53	+0.290	-0.0055	+0.0573
	+10.57	+0.324	-0.0059	+0.0691
	+11.61	+0.356	-0.0061	+0.0817
	+12.66	+0.389	-0.0063	+0.0956
	+0.20	+0.009	-0.0002	+0.0105

(Contd.)

TABLE 2 (Contd.)

M	α	C_L	C_m	C_D
1.82	-2.06	-0.050	+0.0009	+0.0115
	-1.03	-0.023	+0.0003	+0.0103
	0	+0.001	0	+0.0095
	+1.02	+0.024	-0.0002	+0.0106
	+2.06	+0.054	-0.0010	+0.0122
	+3.09	+0.081	-0.0015	+0.0145
	+4.12	+0.112	-0.0022	+0.0181
	+5.16	+0.142	-0.0027	+0.0227
	+6.19	+0.173	-0.0032	+0.0285
	+7.23	+0.203	-0.0036	+0.0355
	+8.27	+0.234	-0.0038	+0.0431
	+9.31	+0.265	-0.0041	+0.0531
	+10.35	+0.294	-0.0043	+0.0635
	+11.39	+0.324	-0.0044	+0.0750
	+12.43	+0.354	-0.0045	+0.0877
	0	+0.001	-0.0001	+0.0092
	-1.08	-0.024	+0.0004	+0.0103
	-0.82	-0.016	+0.0002	+0.0100
	-0.63	-0.018	+0.0004	+0.0101
	-0.42	-0.011	+0.0003	+0.0094
	-0.21	-0.004	+0.0002	+0.0094
	0	+0.001	+0.0001	+0.0092
	+0.20	+0.005	+0.0001	+0.0093
	+0.41	+0.011	+0.0000	+0.0096
	+0.61	+0.015	+0.0001	+0.0101
	+0.82	+0.020	0	+0.0106
	+1.03	+0.027	-0.0002	+0.0107
	+1.23	+0.031	-0.0003	+0.0111
2.00	-2.05	-0.046	+0.0006	+0.0105
	-1.08	-0.022	+0.0001	+0.0086
	0	+0.001	0	+0.0079
	+1.03	+0.027	-0.0002	+0.0089
	+2.05	+0.049	-0.0006	+0.0110
	+3.07	+0.077	-0.0013	+0.0136
	+4.10	+0.103	-0.0018	+0.0171
	+5.13	+0.131	-0.0022	+0.0211
	+6.16	+0.160	-0.0026	+0.0264
	+7.19	+0.189	-0.0029	+0.0328
	+8.22	+0.216	-0.0030	+0.0401
	+9.25	+0.243	-0.0031	+0.0489
	+10.28	+0.271	-0.0032	+0.0585
	+11.31	+0.298	-0.0032	+0.0693
	+12.34	+0.325	-0.0033	+0.0810
	-4.10	-0.105	+0.0018	+0.0160
	-4.10	-0.104	+0.0018	+0.0159
	-3.08	-0.076	+0.0013	+0.0130
	-2.05	-0.049	+0.0007	+0.0105
	-1.04	-0.042	+0.0009	+0.0091
	0	-0.001	0	+0.0081

TABLE 3

RESULTS - WING 10

M	α	C_L	C_m	C_D
0.40	-2.00	-0.099	-0.0003	0.0170
	-1.08	-0.072	+0.0012	0.0143
	-0.01	-0.041	0.0028	0.0123
	1.01	-0.012	0.0043	0.0108
	1.98	+0.017	0.0062	0.0106
	3.05	0.042	0.0078	0.0105
	4.07	0.063	0.0098	0.0111
	5.09	0.084	0.0121	0.0126
	6.12	0.117	0.0145	0.0157
	7.14	0.152	0.0165	0.0200
	8.17	0.185	0.0190	0.0259
	9.20	0.224	0.0216	0.0338
	10.23	0.264	0.0252	0.0438
	11.27	0.307	0.0293	0.0555
	12.31	0.351	0.0333	0.0695
0.70	-2.03	-0.103	0.0003	0.0175
	-1.05	-0.073	0.0017	0.0148
	-0.01	-0.041	0.0032	0.0128
	1.02	-0.012	0.0047	0.0108
	2.00	+0.016	0.0061	0.0103
	3.09	0.044	0.0074	0.0105
	4.12	0.068	0.0095	0.0116
	5.15	0.093	0.0117	0.0137
	6.19	0.122	0.0139	0.0167
	7.23	0.157	0.0159	0.0219
	8.28	0.194	0.0180	0.0275
	9.33	0.236	0.0207	0.0360
	10.39	0.277	0.0238	0.0473
	11.45	0.321	0.0274	0.0600
	12.50	0.367	0.0298	0.0745
0.85	-2.10	-0.108	0.0019	0.0179
	-1.11	-0.078	0.0030	0.0146
	-0.01	-0.034	0.0036	0.0121
	1.03	-0.013	0.0054	0.0113
	2.02	0.016	0.0065	0.0112
	3.11	0.044	0.0078	0.0121
	4.15	0.069	0.0098	0.0130
	5.19	0.096	0.0118	0.0134
	6.24	0.128	0.0139	0.0165
	7.29	0.164	0.0157	0.0214
	8.35	0.205	0.0172	0.0288
	9.41	0.249	0.0193	0.0385
	10.48	0.295	0.0219	0.0503
	11.55	0.341	0.0246	0.0638
	12.62	0.389	0.0270	0.0803

(Contd.)

TABLE 3 (Contd.)

M	α	C_L	C_m	C_D
0.90	-2.09	-0.111	0.0027	0.0179
	-1.05	-0.079	0.0036	0.0146
	-0.01	-0.045	0.0045	0.0123
	1.03	-0.012	0.0058	0.0107
	2.02	+0.014	0.0068	0.0101
	3.11	0.044	0.0078	0.0104
	4.14	0.066	0.0101	0.0114
	5.19	0.098	0.0116	0.0136
	6.23	0.129	0.0136	0.0167
	7.28	0.164	0.0154	0.0214
	8.34	0.207	0.0171	0.0290
	9.40	0.251	0.0186	0.0387
	10.46	0.298	0.0207	0.0506
	11.53	0.346	0.0227	0.0651
	12.59	0.394	0.0246	0.0814
0.94	-2.09	-0.114	0.0032	0.0182
	-1.05	-0.082	0.0039	0.0148
	-0.01	-0.047	0.0047	0.0122
	1.03	-0.014	0.0058	0.0107
	2.02	+0.014	0.0065	0.0102
	3.11	0.044	0.0079	0.0106
	4.15	0.071	0.0095	0.0118
	5.19	0.099	0.0114	0.0139
	6.24	0.130	0.0135	0.0169
	7.29	0.169	0.0147	0.0220
	8.35	0.212	0.0159	0.0298
	9.41	0.258	0.0176	0.0398
	10.47	0.304	0.0189	0.0520
	11.54	0.356	0.0203	0.0672
	12.60	0.404	0.0217	0.0837
0.98	-2.09	-0.122	0.0048	0.0190
	-1.10	-0.085	0.0050	0.0152
	0	-0.048	0.0054	0.0126
	1.03	-0.015	0.0056	0.0112
	2.03	0.016	0.0071	0.0107
	3.12	0.044	0.0081	0.0109
	4.16	0.072	0.0101	0.0121
	5.20	0.099	0.0118	0.0141
	6.25	0.133	0.0136	0.0175
	7.30	0.170	0.0145	0.0228
	8.31	0.218	0.0146	0.0309
	9.41	0.264	0.0148	0.0415
	10.47	0.312	0.0156	0.0540
	11.53	0.362	0.0157	0.0693
	12.59	0.409	0.0166	0.0856

(Contd.)

TABLE 3 (Contd.)

M	α	C_L	C_m	C_D
1.02	-2.07	-0.121	0.0080	0.0208
	-1.08	-0.086	0.0077	0.0176
	0	-0.050	0.0071	0.0145
	1.04	-0.015	0.0071	0.0126
	2.03	0.017	0.0071	0.0125
	2.03	0.017	0.0072	0.0120
	3.12	0.048	0.0074	0.0128
	4.16	0.076	0.0087	0.0145
	5.20	0.108	0.0090	0.0169
	6.24	0.140	0.0106	0.0202
	7.29	0.184	0.0093	0.0267
	8.33	0.228	0.0090	0.0347
	9.38	0.275	0.0084	0.0454
	10.44	0.326	0.0078	0.0588
	11.50	0.370	0.0077	0.0729
	12.55	0.422	0.0084	0.0909
1.42	-1.95	-0.098	+0.0091	+0.0188
	-0.97	-0.066	+0.0083	+0.0156
	+0.12	-0.034	+0.0077	+0.0137
	+1.15	-0.003	+0.0070	+0.0127
	+2.18	+0.027	+0.0064	+0.0127
	+3.22	+0.055	+0.0059	+0.0134
	+4.25	+0.083	+0.0059	+0.0151
	+5.29	+0.112	+0.0056	+0.0176
	+6.33	+0.144	+0.0055	+0.0210
	+7.37	+0.179	+0.0051	+0.0261
	+8.41	+0.217	+0.0041	+0.0340
	+9.46	+0.257	+0.0038	+0.0435
	+10.51	+0.296	+0.0038	+0.0542
	+11.56	+0.334	+0.0038	+0.0666
	+12.61	+0.372	+0.0039	+0.0807
	+0.12	-0.034	+0.0077	+0.0137
1.61	-1.85	-0.083	+0.0078	+0.0173
	-0.87	-0.052	+0.0071	+0.0145
	+0.22	-0.022	+0.0065	+0.0128
	+1.25	+0.007	+0.0049	+0.0120
	+2.28	+0.034	+0.0043	+0.0120
	+3.31	+0.062	+0.0040	+0.0130
	+4.35	+0.087	+0.0038	+0.0147
	+5.38	+0.115	+0.0035	+0.0174
	+6.32	+0.145	+0.0031	+0.0210
	+7.45	+0.176	+0.0028	+0.0257
	+8.49	+0.212	+0.0021	+0.0328
	+9.54	+0.248	+0.0018	+0.0419
	+10.59	+0.285	+0.0018	+0.0524
	+11.64	+0.318	+0.0020	+0.0635
	+12.69	+0.353	+0.0023	+0.0767
	+0.22	-0.023	+0.0056	+0.0127

(Contd.)

TABLE 3 (Contd.)

M	α	C_L	C_m	C_D
1.82	-2.05	-0.080	+0.0070	+0.0164
	-1.07	-0.055	+0.0065	+0.0138
	+0.01	-0.025	+0.0059	+0.0122
	+1.04	+0.001	+0.0055	+0.0114
	+2.07	+0.029	+0.0050	+0.0114
	+3.10	+0.056	+0.0045	+0.0122
	+4.13	+0.080	+0.0043	+0.0137
	+5.17	+0.107	+0.0040	+0.0165
	+6.20	+0.134	+0.0038	+0.0200
	+7.24	+0.164	+0.0035	+0.0245
	+8.28	+0.196	+0.0032	+0.0307
	+9.32	+0.229	+0.0030	+0.0391
	+10.36	+0.261	+0.0032	+0.0486
	+11.41	+0.293	+0.0034	+0.0592
	+12.45	+0.324	+0.0038	+0.0711
	+4.13	+0.079	+0.0044	+0.0136
	+4.34	+0.084	+0.0044	+0.0142
	+4.55	+0.090	+0.0043	+0.0148
	+4.75	+0.095	+0.0043	+0.0153
	+4.96	+0.101	+0.0042	+0.0158
	+5.17	+0.106	+0.0041	+0.0164
	+0.01	-0.028	+0.0063	+0.0123
2.00	-2.04	-0.079	+0.0066	+0.0157
	-1.07	-0.053	+0.0061	+0.0135
	+0.01	-0.026	+0.0056	+0.0116
	+1.04	+0	+0.0051	+0.0106
	+2.06	+0.026	+0.0046	+0.0104
	+3.08	+0.051	+0.0043	+0.0109
	+4.11	+0.074	+0.0040	+0.0129
	+5.13	+0.099	+0.0038	+0.0156
	+6.16	+0.125	+0.0035	+0.0188
	+7.19	+0.153	+0.0032	+0.0233
	+8.22	+0.183	+0.0030	+0.0289
	+9.25	+0.211	+0.0031	+0.0360
	+10.29	+0.241	+0.0032	+0.0450
	+11.32	+0.270	+0.0037	+0.0547
	+12.36	+0.298	+0.0039	+0.0655
	+4.11	+0.076	+0.0041	+0.0127
	+4.11	+0.074	+0.0041	+0.0122
	+4.62	+0.087	+0.0039	+0.0139
	+5.13	+0.100	+0.0038	+0.0155
	+5.65	+0.113	+0.0036	+0.0173
	+3.60	+0.063	+0.0041	+0.0116
	+0.01	-0.027	+0.0057	+0.0116

TABLE 4

RESULTS - WING 11

M	α	C_L	C_m	C_D
0.40	-2.04	-0.063	-0.0022	0.0118
	-1.52	-0.036	-0.0006	0.0105
	0	-0.009	0.0012	0.0095
	1.02	+0.013	0.0031	0.0098
	1.99	0.028	0.0053	0.0105
	3.06	0.057	0.0069	0.0122
	4.08	0.092	0.0087	0.0145
	5.11	0.125	0.0102	0.0185
	6.13	0.156	0.0133	0.0234
	7.16	0.193	0.0155	0.0303
	8.19	0.224	0.0189	0.0372
	9.22	0.264	0.0219	0.0472
	10.26	0.309	0.0246	0.0592
	11.30	0.355	0.0286	0.0737
	12.33	0.394	0.0328	0.0882
0.70	-2.07	-0.068	-0.0018	0.0121
	-1.08	-0.041	-0.0001	0.0106
	0	-0.013	0.0016	0.0097
	1.03	0.011	0.0032	0.0097
	2.01	0.034	0.0049	0.0104
	3.10	0.063	0.0065	0.0125
	4.14	0.094	0.0086	0.0154
	5.18	0.127	0.0105	0.0184
	6.22	0.163	0.0129	0.0237
	7.26	0.200	0.0147	0.0313
	8.31	0.233	0.0174	0.0386
	9.37	0.282	0.0198	0.0502
	10.42	0.324	0.0229	0.0628
	11.48	0.368	0.0260	0.0770
	12.54	0.415	0.0282	0.0938
0.85	-2.09	-0.072	-0.0011	0.0125
	-1.09	-0.043	0.0003	0.0107
	0	-0.014	0.0016	0.0097
	1.04	0.011	0.0034	0.0099
	2.03	0.037	0.0050	0.0104
	3.12	0.065	0.0066	0.0122
	4.17	0.098	0.0081	0.0147
	5.22	0.133	0.0098	0.0189
	6.27	0.171	0.0115	0.0246
	7.33	0.211	0.0133	0.0326
	8.39	0.252	0.0141	0.0416
	9.45	0.296	0.0172	0.0531
	10.51	0.340	0.0193	0.0661
	11.58	0.387	0.0214	0.0815
	12.65	0.432	0.0260	0.0986

(Contd.)

TABLE 4 (Contd.)

M	α	C_L	C_m	C_D
0.90	-2.08	-0.073	-0.0010	0.0125
	-1.09	-0.043	+0.0003	0.0106
	0	-0.015	0.0019	0.0098
	1.04	0.011	0.0033	0.0095
	2.03	0.036	0.0051	0.0107
	3.12	0.066	0.0066	0.0119
	4.16	0.099	0.0080	0.0147
	5.21	0.134	0.0093	0.0189
	6.26	0.173	0.0112	0.0250
	7.31	0.213	0.0122	0.0327
	8.37	0.255	0.0139	0.0419
	9.43	0.299	0.0155	0.0535
	10.49	0.344	0.0174	0.0670
	11.55	0.389	0.0190	0.0823
	12.62	0.439	0.0207	0.1005
0.94	-2.08	-0.078	-0.0009	0.0125
	-1.09	-0.045	0	0.0107
	0	-0.015	0.0014	0.0098
	1.04	0.011	0.0030	0.0094
	2.03	0.038	0.0047	0.0105
	3.12	0.067	0.0061	0.0120
	4.17	0.102	0.0074	0.0151
	5.22	0.137	0.0088	0.0194
	6.27	0.175	0.0102	0.0251
	7.32	0.216	0.0112	0.0331
	8.38	0.259	0.0124	0.0428
	9.43	0.305	0.0135	0.0546
	10.49	0.348	0.0150	0.0680
	11.55	0.398	0.0159	0.0844
	12.61	0.447	0.0165	0.1028
0.98	-2.08	-0.077	-0.0003	0.0130
	-1.09	-0.046	0.0006	0.0110
	0	-0.016	0.0015	0.0098
	1.05	0.010	0.0033	0.0096
	2.03	0.036	0.0048	0.0106
	3.13	0.069	0.0059	0.0124
	4.17	0.101	0.0072	0.0151
	5.22	0.140	0.0080	0.0199
	6.27	0.180	0.0089	0.0261
	7.32	0.223	0.0092	0.0344
	8.37	0.266	0.0096	0.0423
	9.43	0.312	0.0098	0.0565
	10.48	0.358	0.0098	0.0707
	11.53	0.406	0.0095	0.0870
	12.59	0.458	0.0086	0.1059

(Contd.)

TABLE 4 (Contd.)

M	α	C_L	C_m	C_D
1.02	-2.07	-0.086	0.0025	0.0158
	-1.08	-0.049	0.0025	0.0133
	+0.01	-0.017	0.0027	0.0123
	1.05	0.009	0.0037	0.0115
	2.03	0.038	0.0045	0.0128
	3.12	0.071	0.0048	0.0147
	4.17	0.108	0.0051	0.0178
	5.21	0.145	0.0048	0.0228
	6.26	0.188	0.0047	0.0295
	7.30	0.231	0.0042	0.0377
	8.35	0.275	0.0042	0.0479
	9.40	0.317	0.0047	0.0593
	10.46	0.360	0.0047	0.0730
	11.51	0.405	0.0047	0.0889
	12.57	0.455	0.0048	0.1072
1.42	-0.39	-0.022	+0.0049	+0.0122
	+0.13	-0.011	+0.0048	+0.0121
	+1.16	+0.017	+0.0046	+0.0120
	+2.19	+0.045	+0.0042	+0.0129
	+3.23	+0.074	+0.0038	+0.0148
	+4.27	+0.108	+0.0034	+0.0178
	+5.31	+0.141	+0.0029	+0.0221
	+6.35	+0.176	+0.0026	+0.0278
	+7.39	+0.211	+0.0022	+0.0349
	+8.44	+0.247	+0.0021	+0.0434
	+9.48	+0.284	+0.0018	+0.0539
	+10.53	+0.320	+0.0017	+0.0653
	+11.58	+0.356	+0.0020	+0.0783
	+12.63	+0.392	+0.0018	+0.0927
	+0.13	-0.010	+0.0047	+0.0118
1.61	-1.84	-0.059	+0.0052	+0.0131
	-0.86	-0.030	+0.0048	+0.0119
	+0.23	-0.004	+0.0047	+0.0113
	+1.26	+0.022	+0.0044	+0.0113
	+2.29	+0.048	+0.0040	+0.0125
	+3.22	+0.074	+0.0035	+0.0140
	+4.35	+0.106	+0.0030	+0.0170
	+5.39	+0.137	+0.0026	+0.0210
	+6.43	+0.170	+0.0022	+0.0266
	+7.47	+0.203	+0.0019	+0.0334
	+8.52	+0.236	+0.0017	+0.0413
	+9.56	+0.269	+0.0018	+0.0506
	+10.61	+0.303	+0.0017	+0.0617
	+11.65	+0.335	+0.0018	+0.0735
	+12.70	+0.367	+0.0020	+0.0868
	+0.27	-0.005	+0.0047	+0.0113

(Contd.)

TABLE 4 (Contd.)

M	α	C_L	C_m	C_D
1.82	-1.99	-0.060	+0.0052	+0.0129
	-1.06	-0.031	+0.0048	+0.0112
	-0.44	-0.018	+0.0045	+0.0107
	+0.02	-0.007	+0.0045	+0.0104
	+0.54	+0.006	+0.0043	+0.0102
	+1.05	+0.018	+0.0042	+0.0104
	+1.57	+0.030	+0.0040	+0.0109
	+2.08	+0.044	+0.0037	+0.0117
	+2.65	+0.056	+0.0035	+0.0124
	+3.11	+0.071	+0.0032	+0.0132
	+4.15	+0.099	+0.0027	+0.0159
	+5.18	+0.128	+0.0024	+0.0199
	+6.22	+0.159	+0.0021	+0.0250
	+7.26	+0.190	+0.0019	+0.0313
	+8.30	+0.220	+0.0017	+0.0386
	+9.39	+0.249	+0.0018	+0.0473
	+10.38	+0.280	+0.0019	+0.0573
	+11.47	+0.310	+0.0020	+0.0687
	+12.46	+0.340	+0.0023	+0.0808
	+0.02	-0.008	+0.0044	+0.0104
2.00	-1.99	-0.063	+0.0047	+0.0122
	-1.06	-0.036	+0.0043	+0.0106
	-0.50	-0.023	+0.0041	+0.0101
	+0.01	-0.013	+0.0041	+0.0097
	+0.53	0	+0.0041	+0.0088
	+1.04	+0.012	+0.0040	+0.0091
	+1.55	+0.023	+0.0040	+0.0097
	+2.06	+0.037	+0.0037	+0.0105
	+2.58	+0.047	+0.0036	+0.0112
	+3.09	+0.060	+0.0033	+0.0122
	+3.09	+0.060	+0.0033	+0.0124
	+4.11	+0.087	+0.0028	+0.0149
	+5.14	+0.115	+0.0025	+0.0185
	+6.17	+0.142	+0.0022	+0.0230
	+7.20	+0.171	+0.0021	+0.0289
	+8.23	+0.198	+0.0022	+0.0355
	+9.26	+0.226	+0.0023	+0.0432
	+10.30	+0.254	+0.0024	+0.0523
	+11.33	+0.280	+0.0026	+0.0621
	+12.36	+0.308	+0.0029	+0.0735
	+0.01	-0.012	+0.0041	+0.0095
	+0.01	-0.012	+0.0041	+0.0095
	+0.53	-0.001	+0.0042	+0.0087

SYMBOLS

A	aspect ratio
C_L	lift coefficient
C_D	drag coefficient
C_m	pitching moment coefficient moment/$qS\bar{\bar{c}}$ referred to $0.66\ c_o$
$\bar{\bar{c}}$	aerodynamic mean chord
c_o	root chord
M	Mach number
p	planform parameter $= S/2c_o\ S_T$
q	free stream kinetic pressure
R	Reynolds number
S	wing area
S_T	wing semi-span
x, y, z	coordinates non-dimensionalised w.r.t. c_o
α	angle of incidence
$\bar{\alpha}$	attachment incidence
β	$\sqrt{M^2 - 1}$

Superscript - attachment conditions

REFERENCES

No.	Author	Title, etc.
1	L.C. Squire	An experimental investigation at supersonic speeds of the characteristics of two gothic wings, one plane and one cambered. A.R.C. R & M 3211 (1959)
2	L.C. Squire	Further experimental investigations of the characteristics of cambered gothic wings at Mach numbers from 0.4 to 2.0. A.R.C. R & M 3310 (1961)
3	L.C. Squire	The characteristics of some slender cambered gothic wings at Mach numbers from 0.4 to 2.0. A.R.C. R & M 3370 (1962)
4	A.L. Courtney A.O. Ormerod	Pressure plotting and force tests at Mach numbers up to 2.8 on an uncambered slender wing of $p = \frac{1}{2}$, $S/c_o = \frac{1}{4}$. ("Handley Page ogee") A.R.C. R & M 3361 (1961)
5	C.R. Taylor	Measurements, at Mach numbers up to 2.8, of the longitudinal characteristics of one plane and three cambered slender ogee wings. A.R.C. R & M 3328 (1961)
6	J. Weber	Design of warped slender wings with the attachment line along the leading-edge. A.R.C. R & M 3406 (1957)
7	A.L. Courtney	Some calculations of shape, pressure distribution and drag due to lift for a "mild ogee" wing with prescribed centre of pressure position. R.A.E. Tech. Note Aero 2655, (A.R.C. 21954) (1959)

REFERENCES (Contd.)

No.	Author	Title, etc.
8	M.S. Igglesden	Tabulated lift, drag and pitching moment data from wind tunnel tests on 30 slender wings of ogee and other planforms with various thickness distributions at M = 1.41, 1.61 and 1.91. R.A.E. Tech. Note Aero 2694, (A.R.C. 22709) (1960)
9	D.G. Mabey	Roughness criteria and drag penalties for bands of distributed roughness on two slender wings at supersonic speeds. A.R.C. C.P. 738 (1963)
10	K.W. Mangler J.H.B. Smith	Calculation of the flow past slender delta wings with leading-edge separations. R.A.E. Report Aero 2593, Proc. Roy. Soc. (1957)
11	J.H.B. Smith	A theory of the separated flow from the curved leading-edge of a slender wing. A.R.C. R & M 3116 (1957)
12	H.W. Carlson	Aerodynamic characteristics at Mach number of 2.05 of a series of highly swept arrow wings employing various degrees of twist and camber. NASA Tech. Memo X332, (1960)
13	A.L. Courtney	A collection of data on the lift-dependent drag on uncambered slender wings at supersonic speeds. A.R.C. C.P. 757 (1960)
14	I. McGregor	Development of the vapour screen method of flow visualisation in the 3ft × 3ft tunnel at R.A.E. Bedford. Tech. Note Aero 2709, (1960)

REFERENCES (Contd.)

No.	Author	Title, etc.
15	D. Pierce	Photographic evidence of the formation and growth of vorticity behind plates accelerated from rest in still air. Journ. Fluid Mech. 11, 460, (1961)
16	L.C. Squire J.G. Jones A. Stanbrook	An experimental investigation of the characteristics of some plane and cambered 65° delta wings at Mach numbers from 0.7 to 2.0. A.R.C. R & M 3305 (1961)

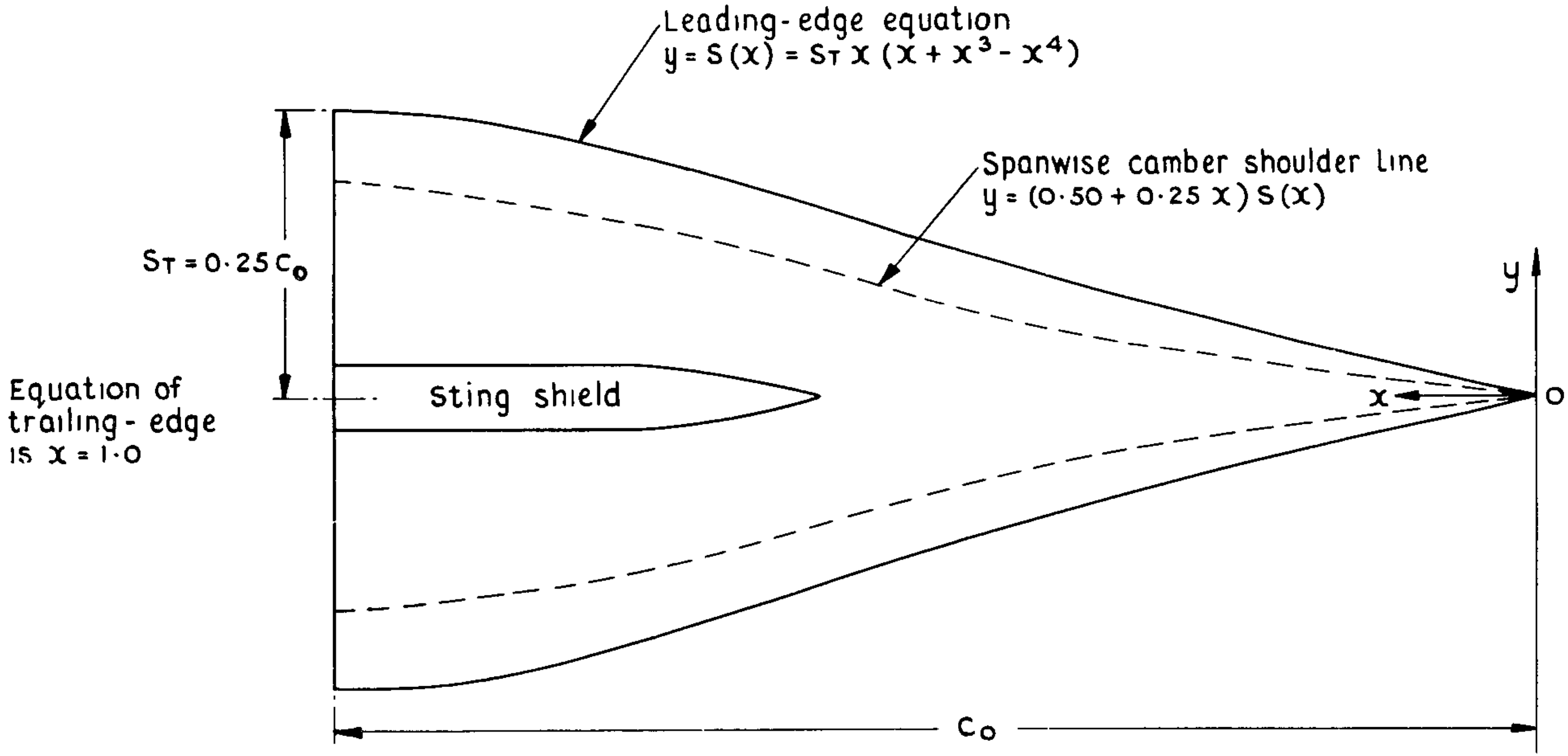

Fig. 1 Planform of wings

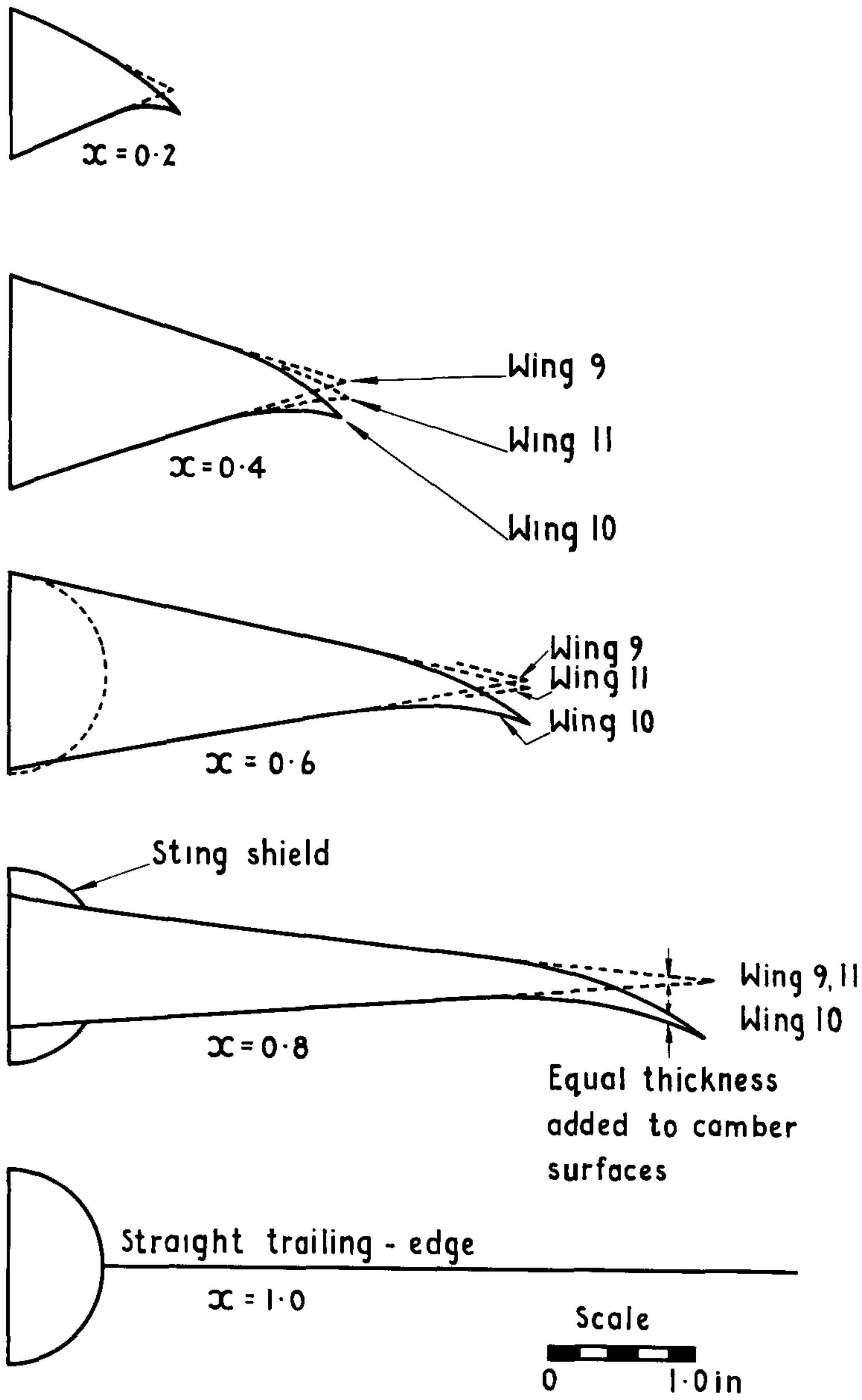

Fig. 2 Sections of wings

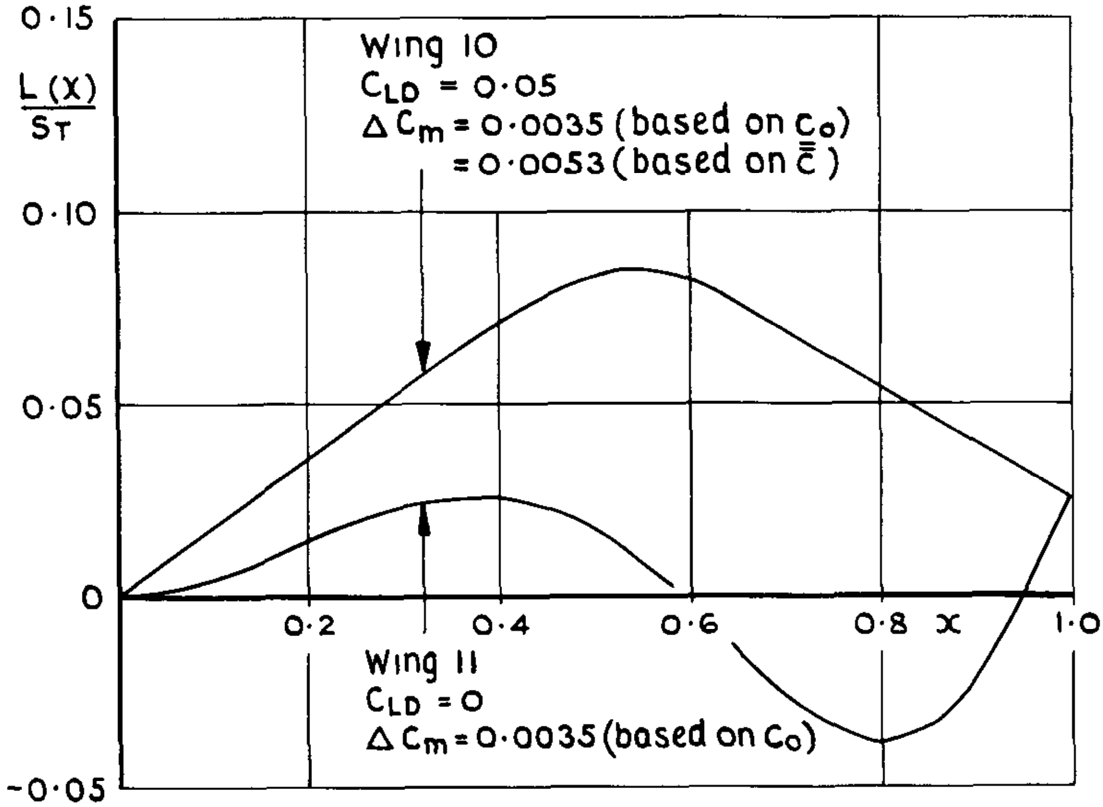

Fig 3 Design chordwise variation of cross-load: Wings 10 and 11

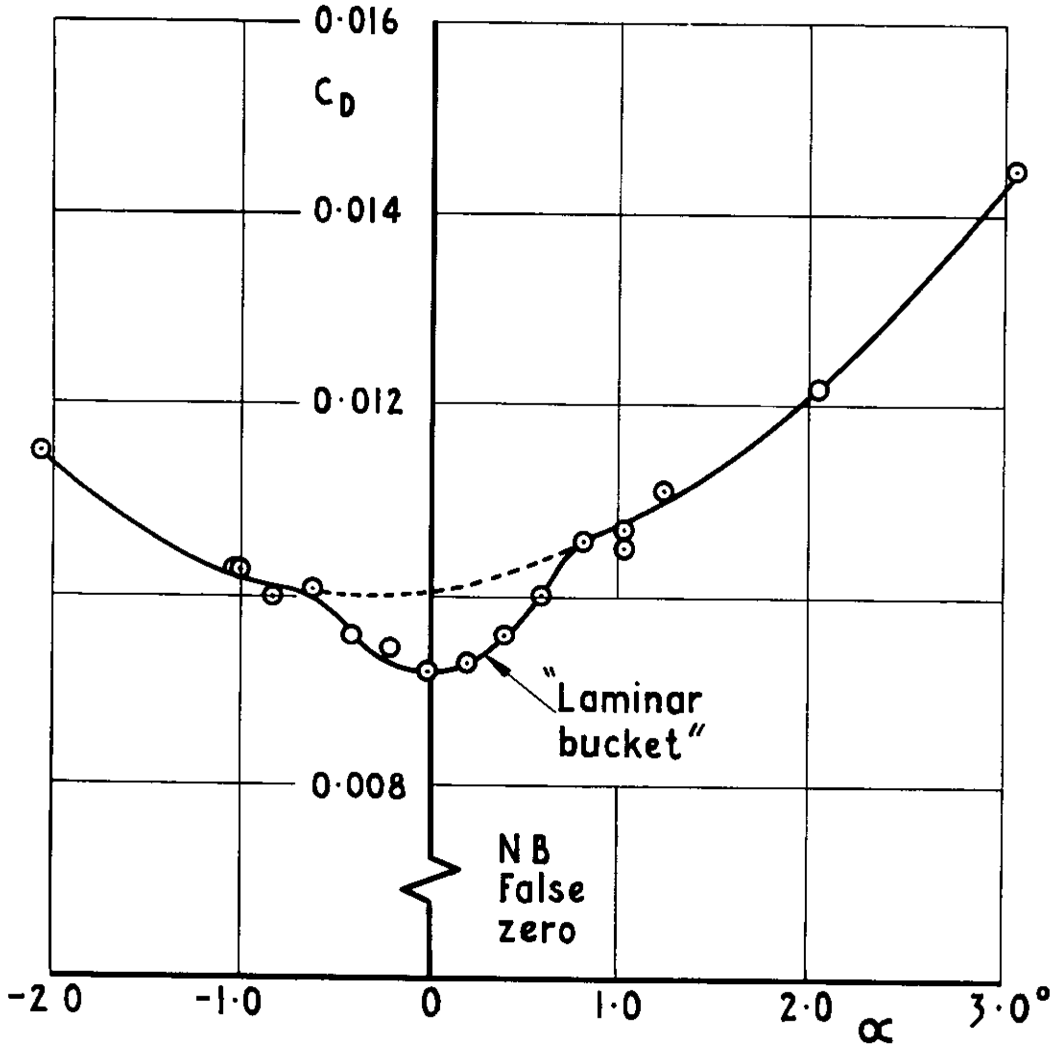

Fig.4 Wing 9. Variation of drag coefficient with incidence near attachment, M = 1·8. Carborundum 0·007 in high

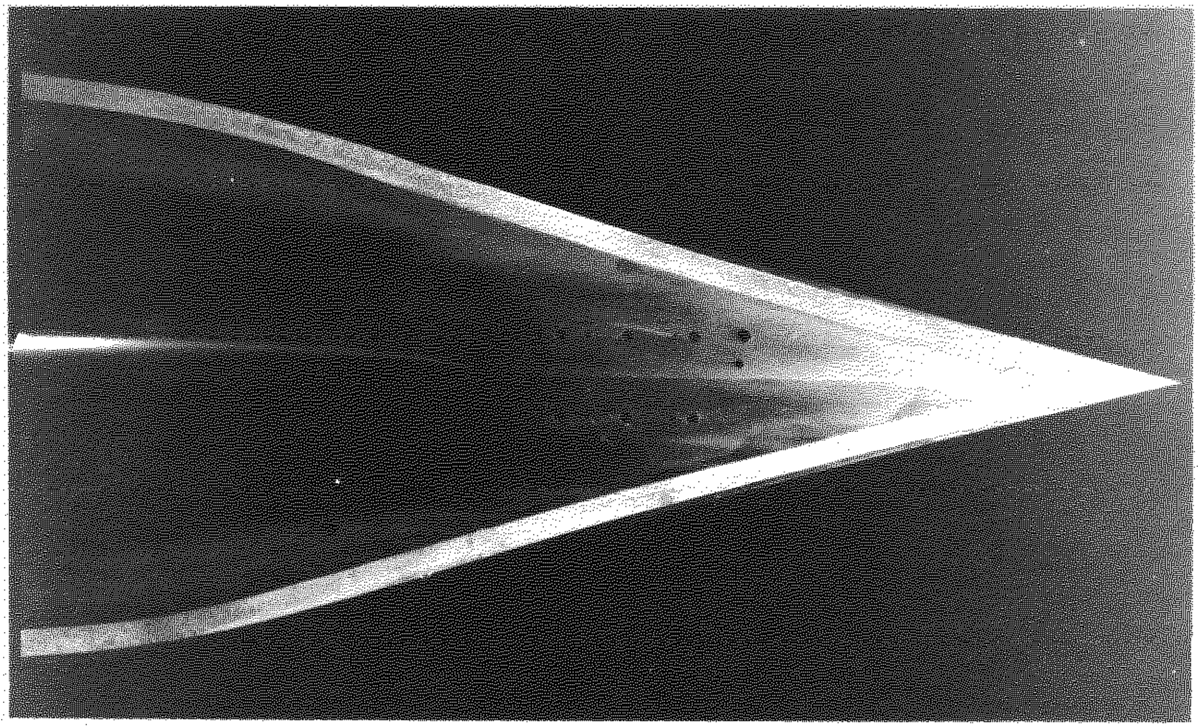

(a) TOP SURFACE

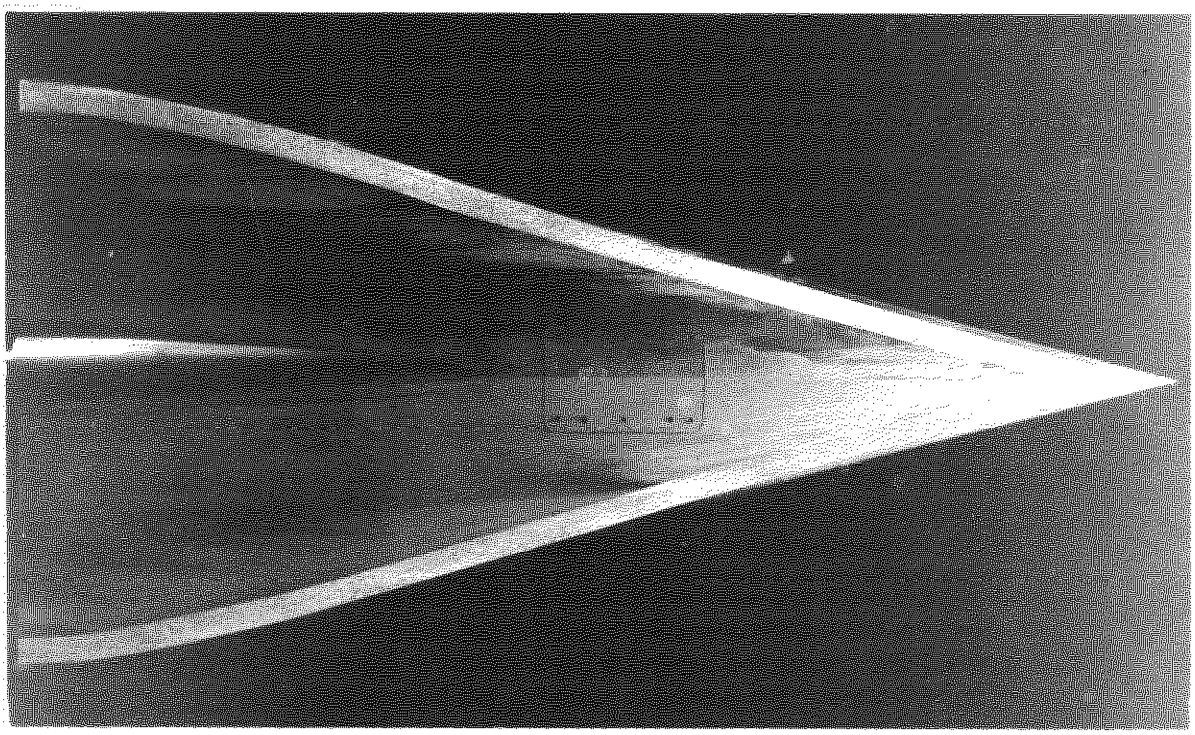

(b) BOTTOM SURFACE

Fig.5 Azo benzene photographs showing transitional boundary layer. Wing 9. M = 2·0 α= 0° carborundum 0·007" high

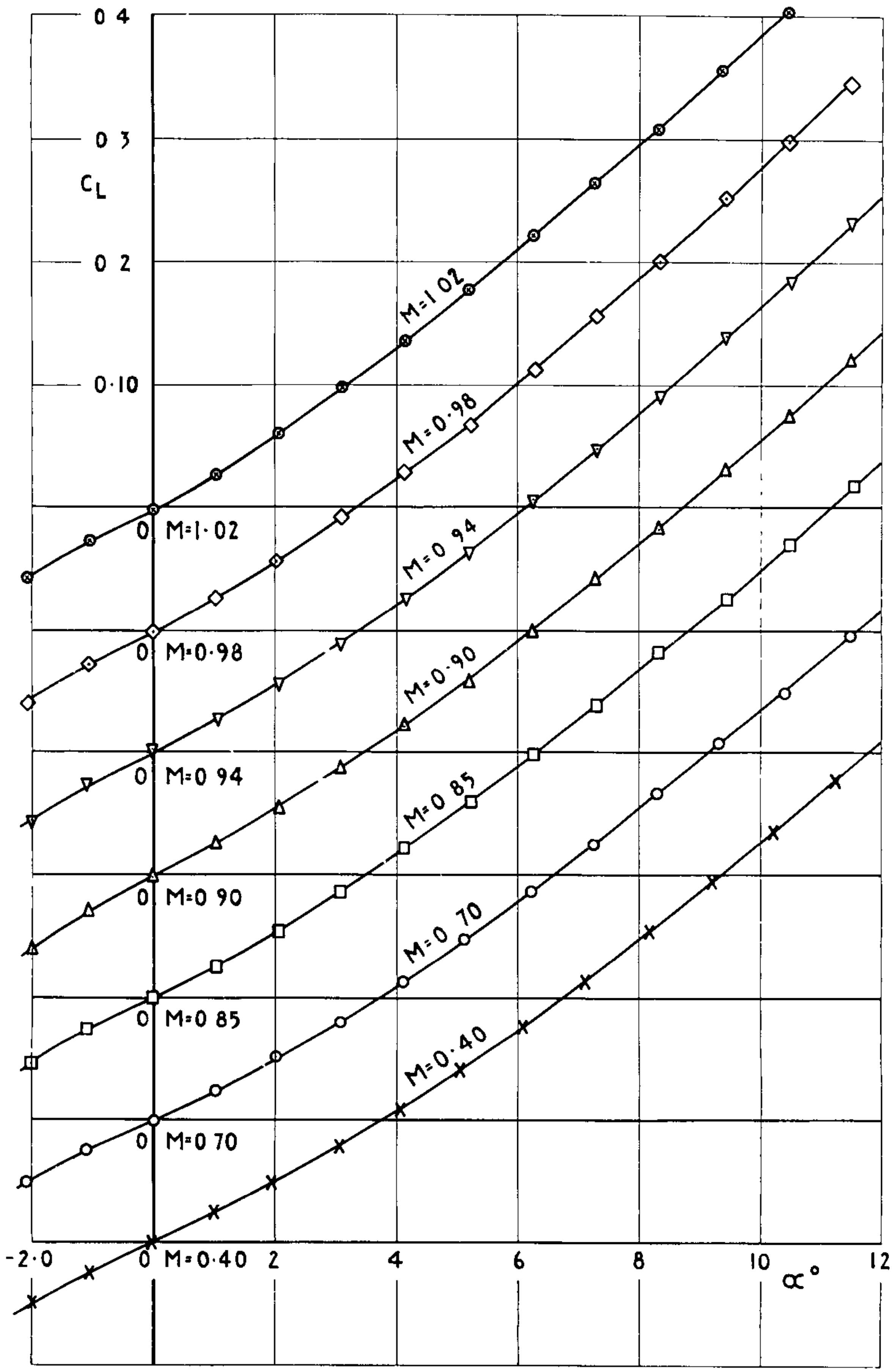

a M=0·40 to 1 02

Fig.6 Wing 9. Variation of lift coefficient with incidence

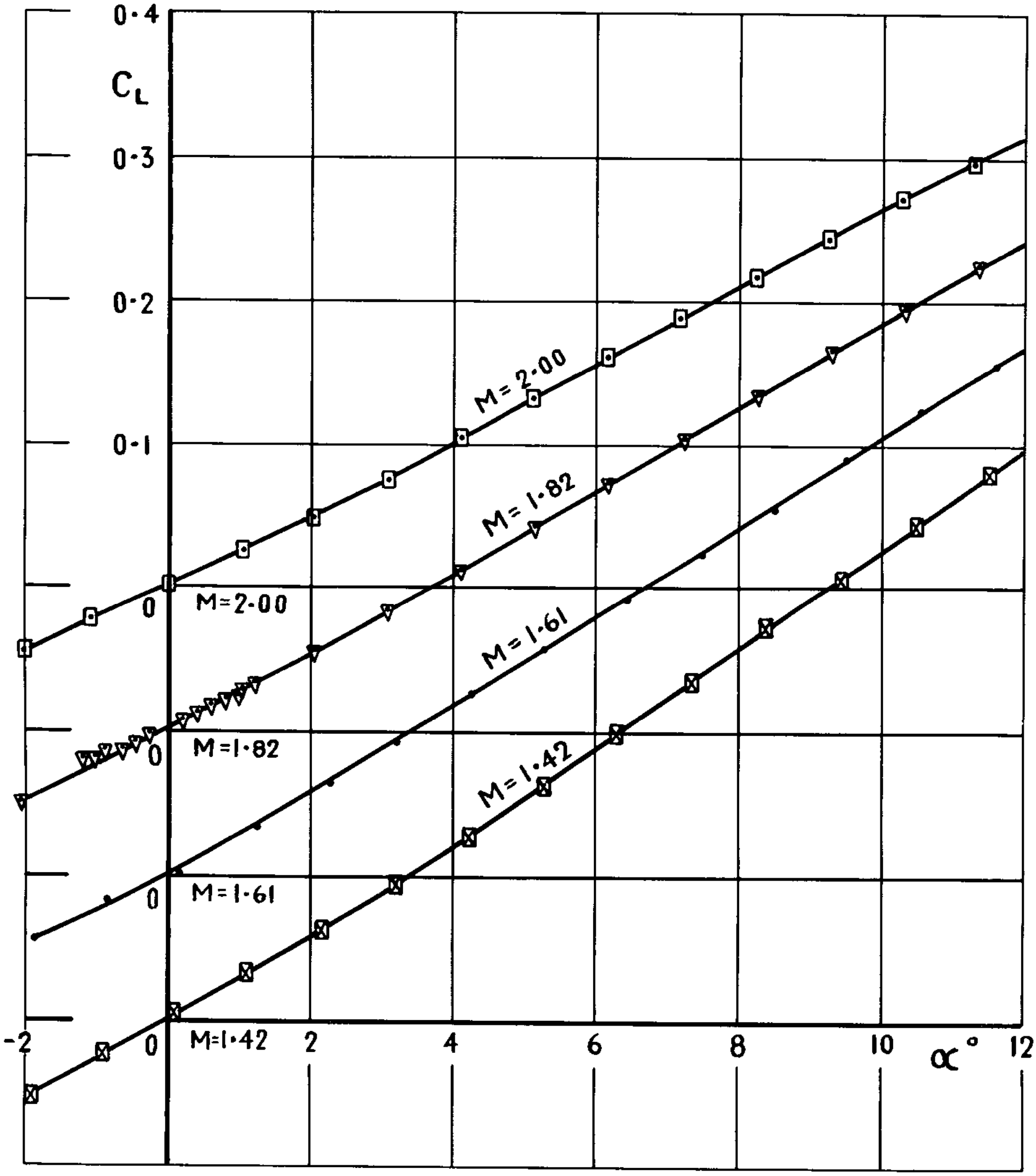

b M = 1·42 to 2·00

Fig. 6 contd.

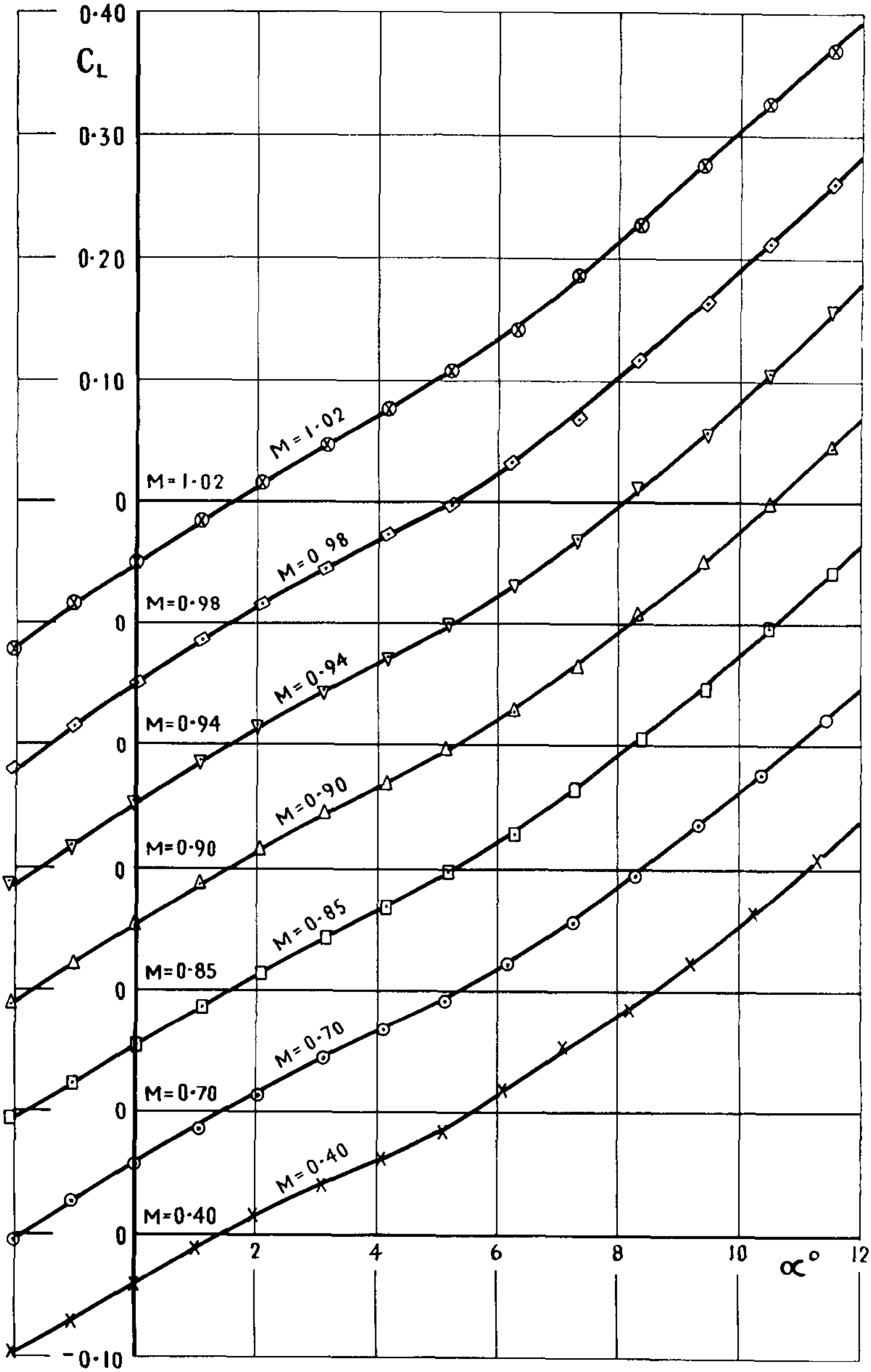

a M = 0·40 to 1·02

Fig. 7 Wing 10. Variation of lift coefficient with incidence

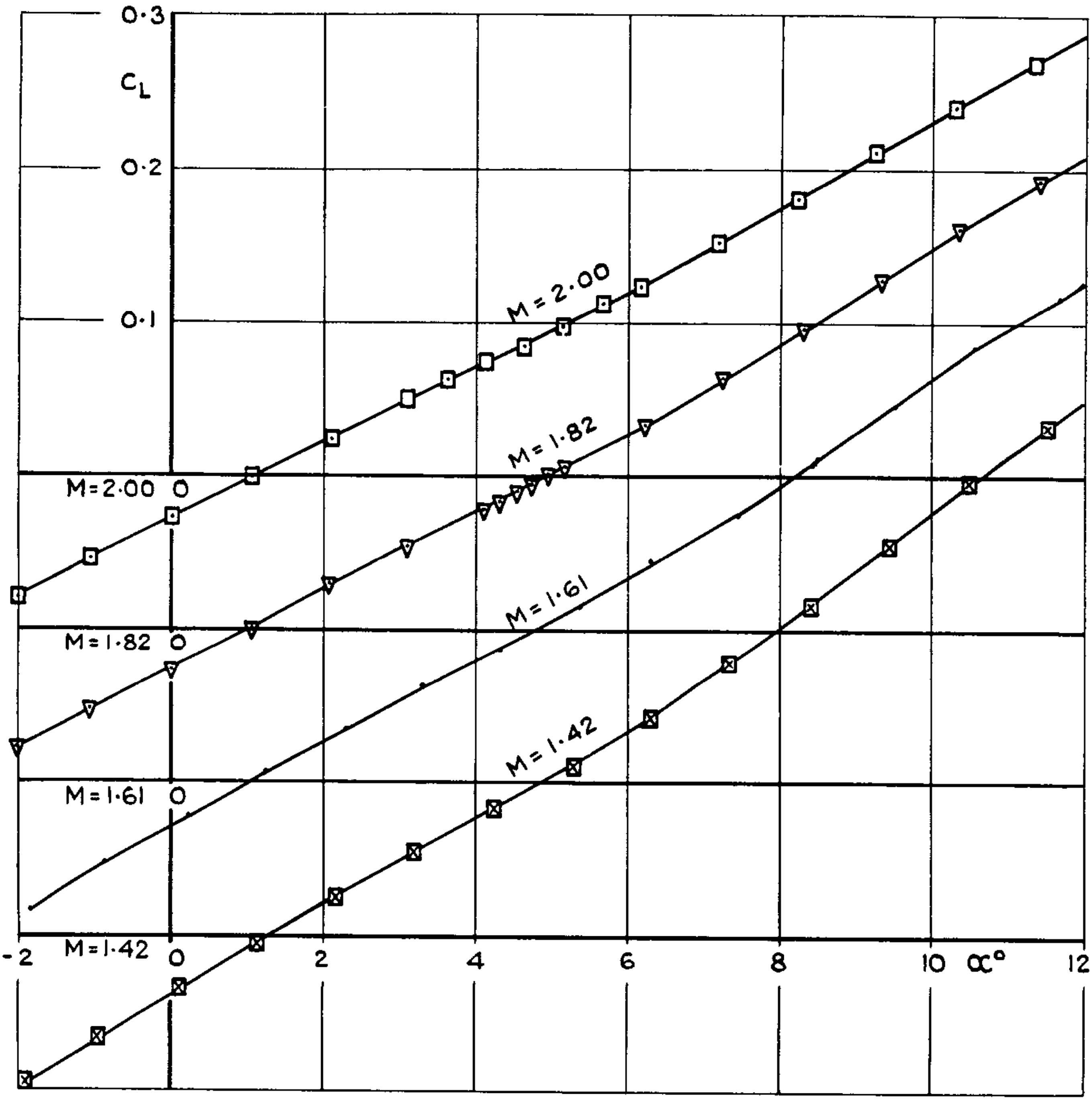

b M = 1·42 to 2·00

Fig 7 contd.

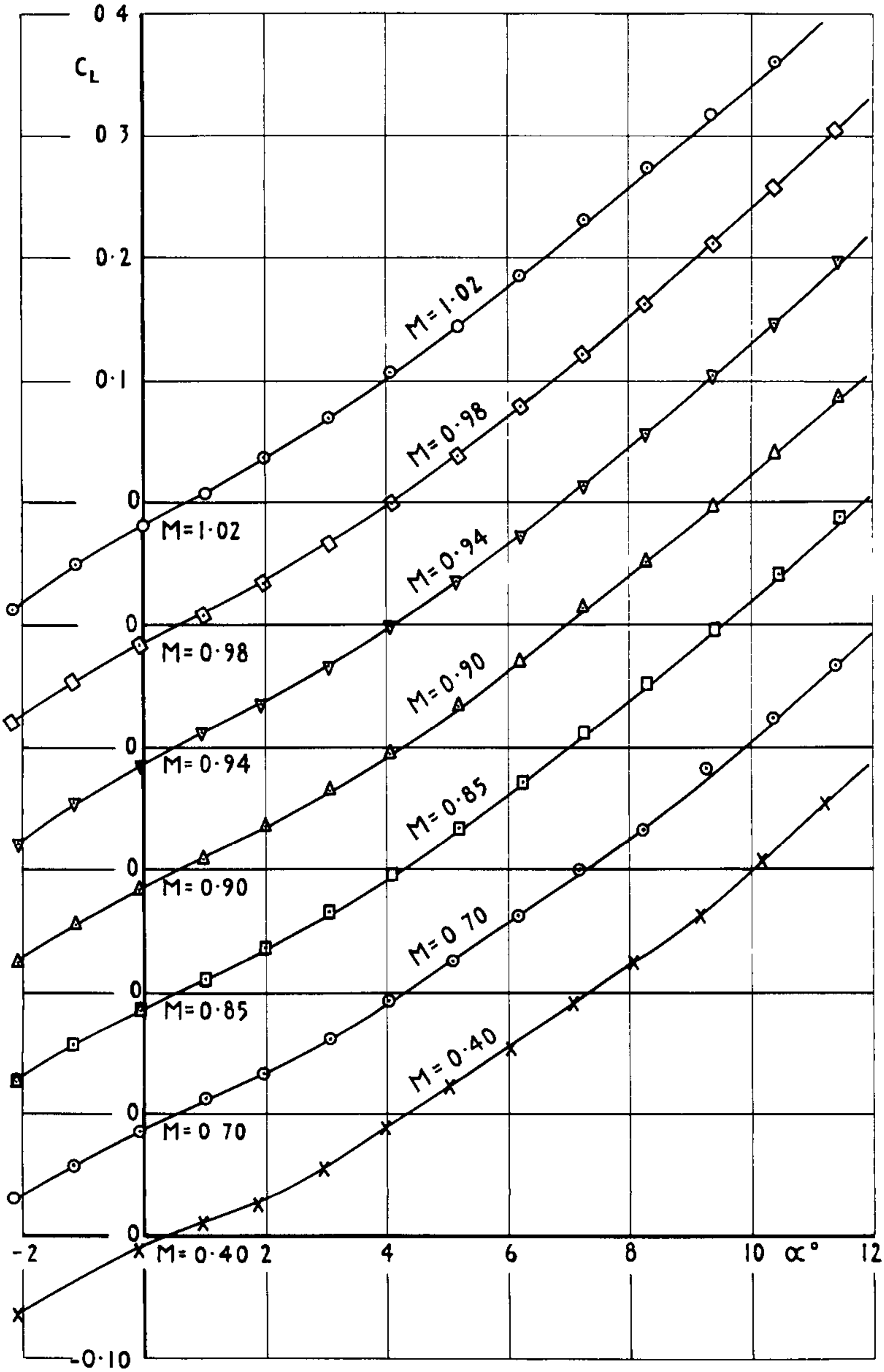

a M=0·40 to 1·02

Fig. 8 Wing II. Variation of lift coefficient with incidence

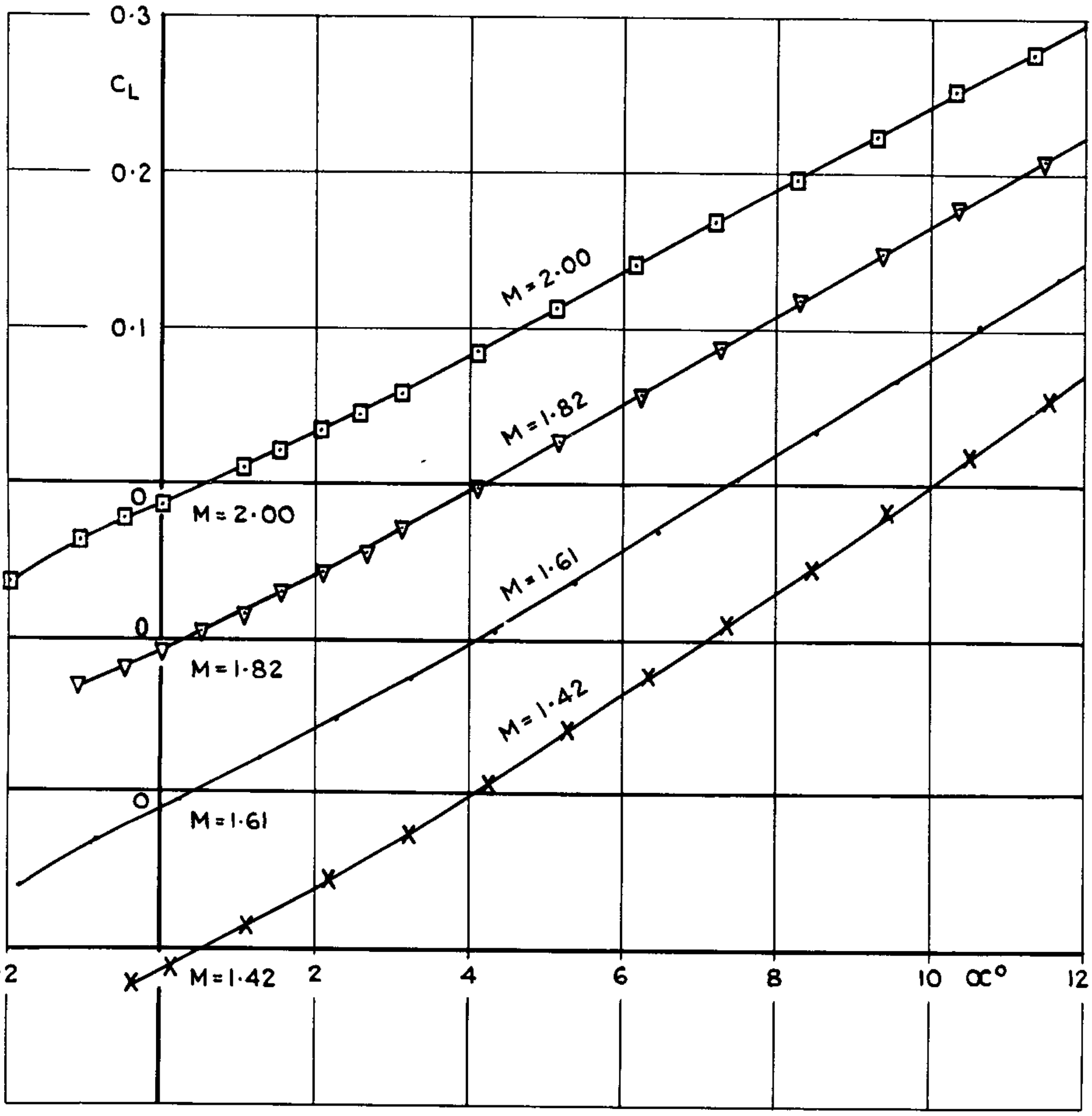

b M = 1·42 to 2·00

Fig. 8 contd.

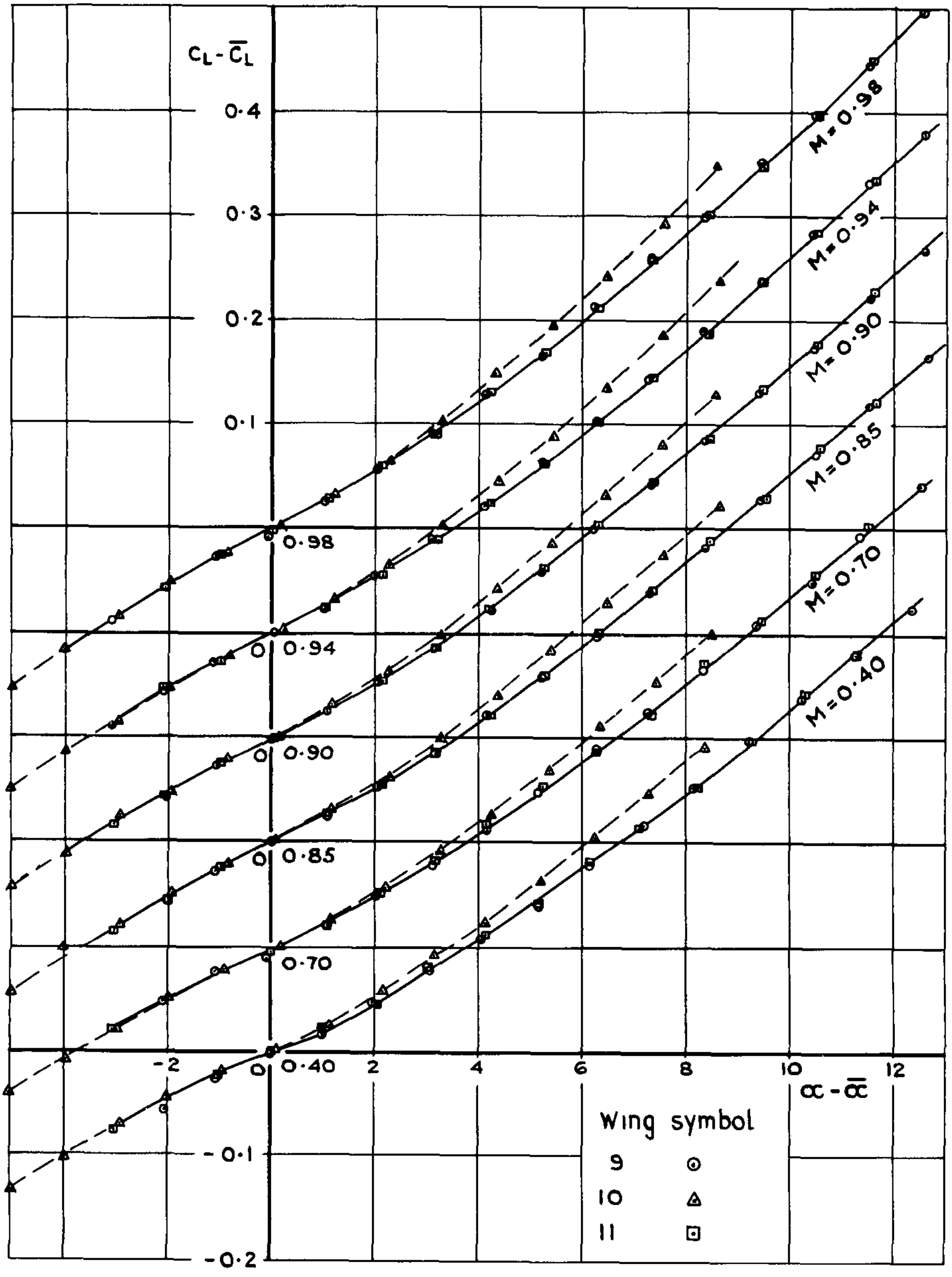

a M=0·40 to M=0·98

Fig. 9 Wings 9-11. Comparison of lift development from the attachment incidence

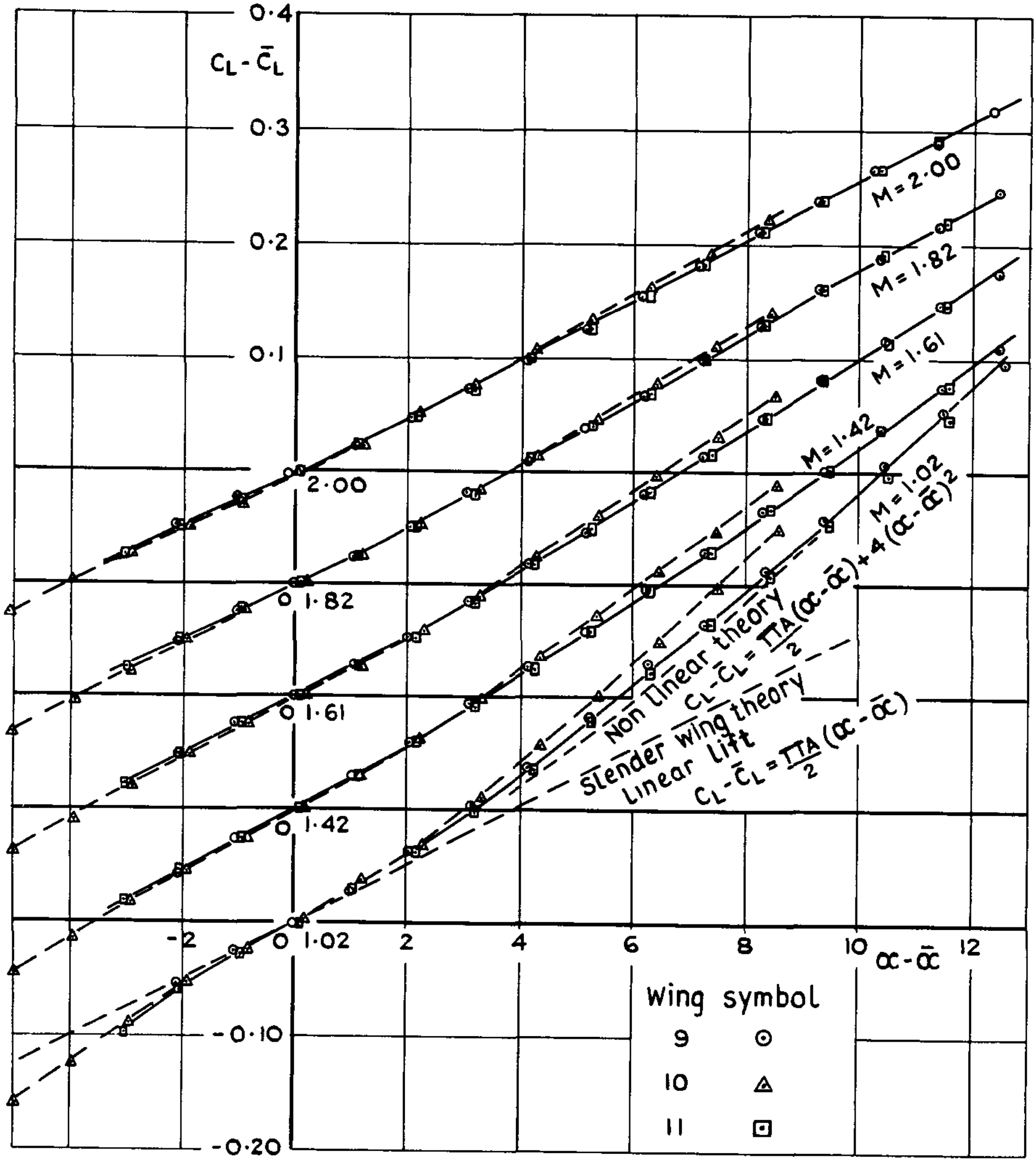

b M = 1·02 to M = 2·00

Fig. 9 contd.

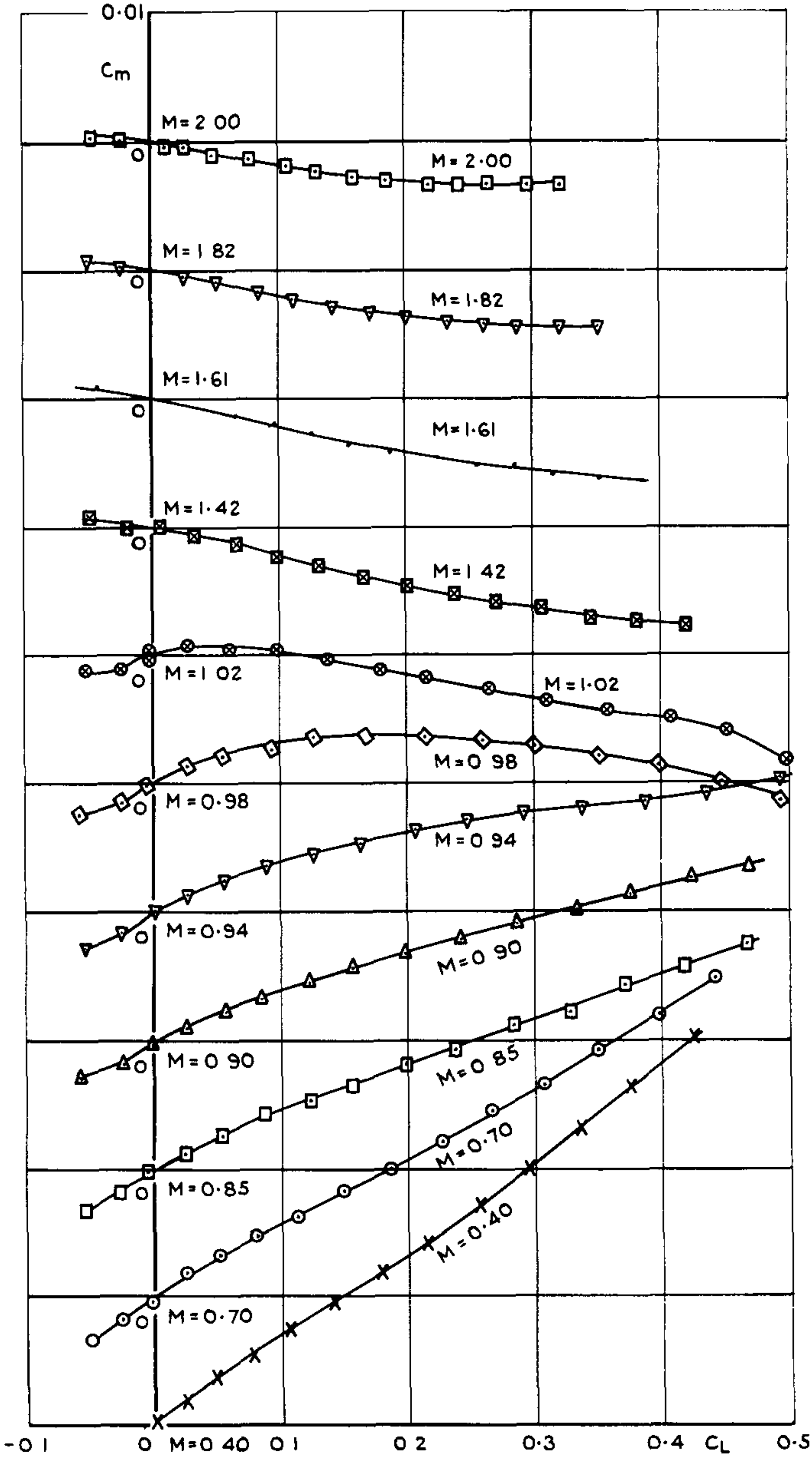

Fig. 10 Wing 9. Variation of pitching moment coefficient with lift coefficient

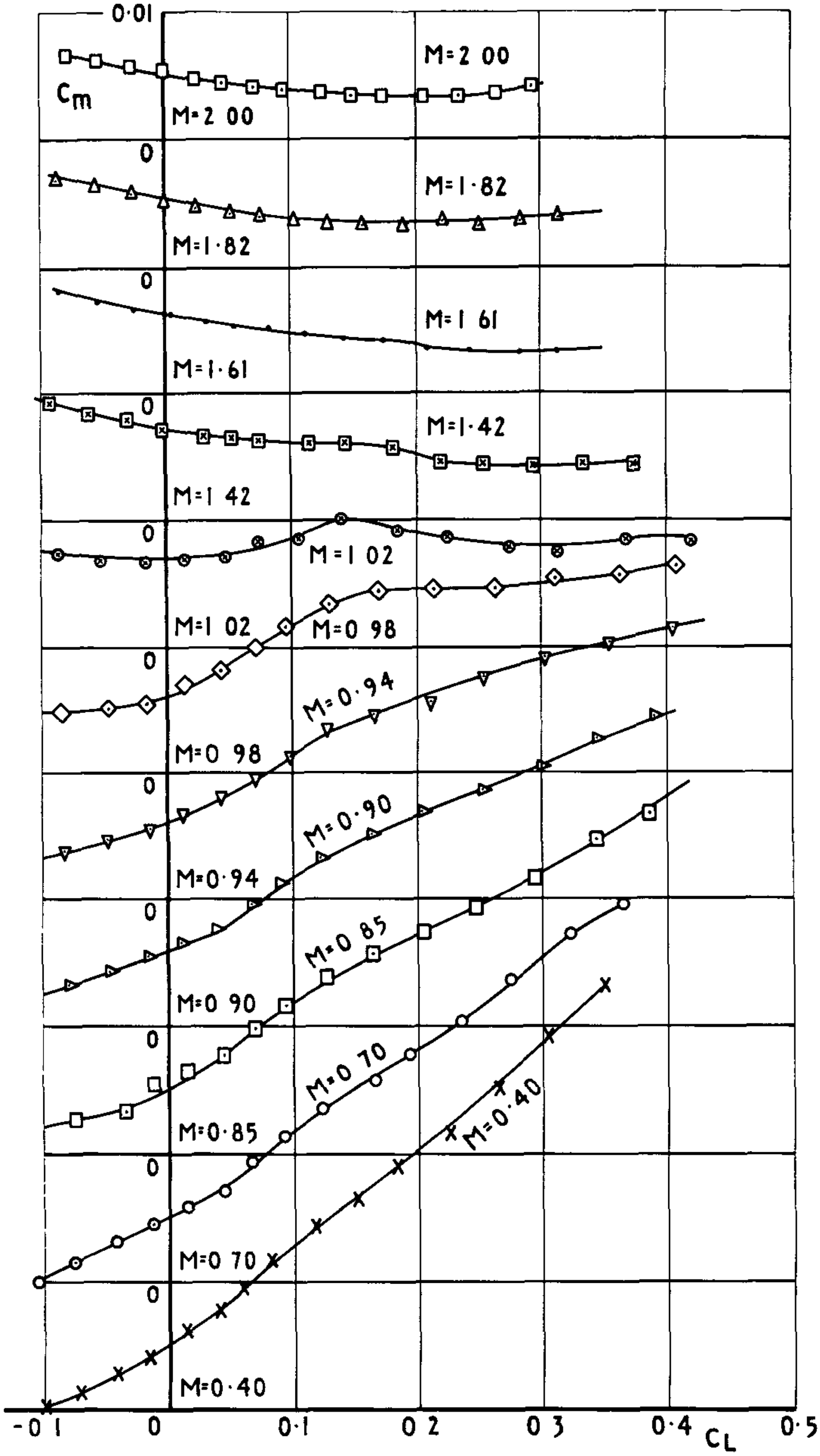

Fig. 11 Wing 10. Variation of pitching moment coefficient with lift coefficient

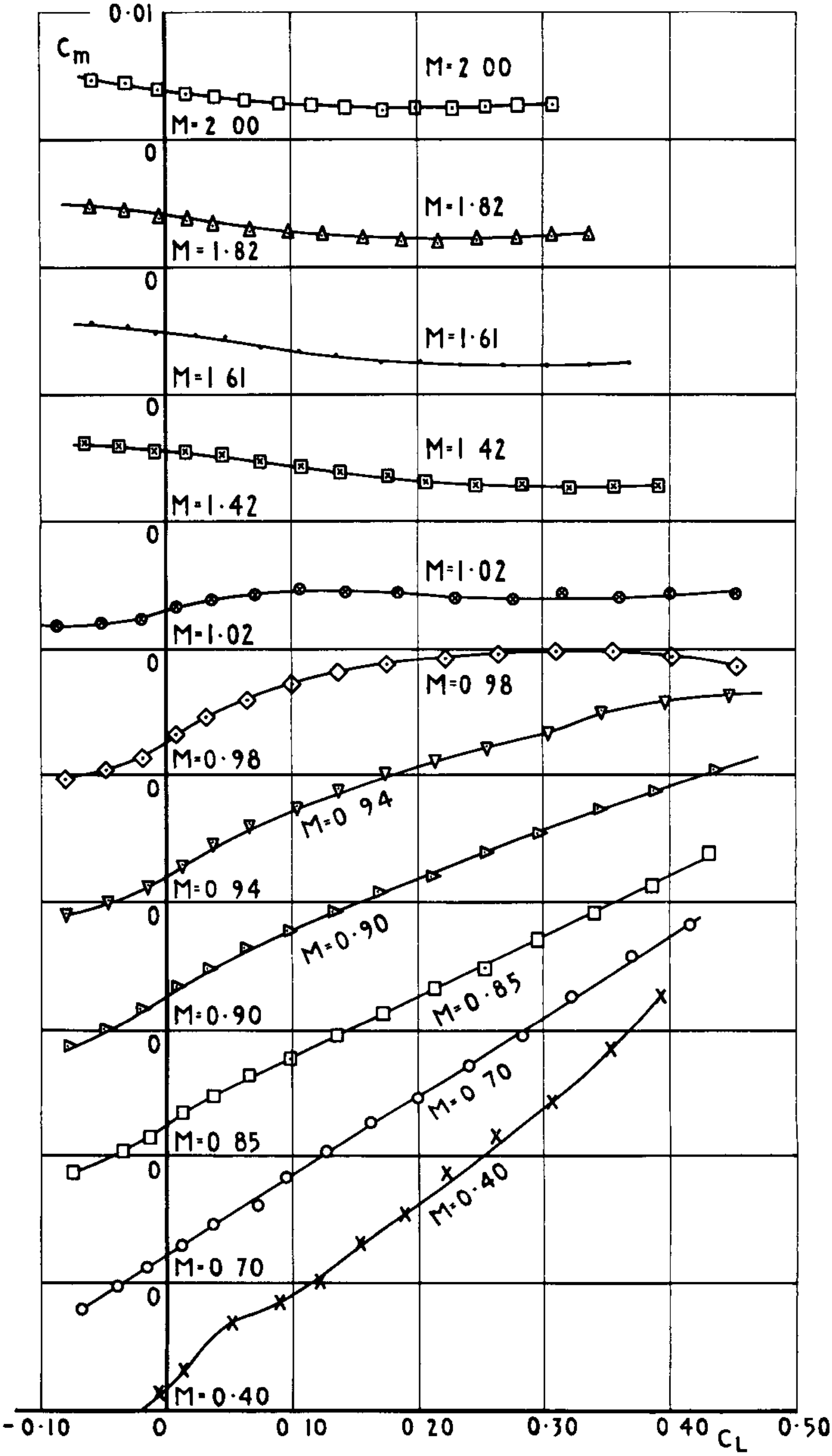

Fig. 12 Wing II. Variation of pitching moment coefficient with lift coefficient

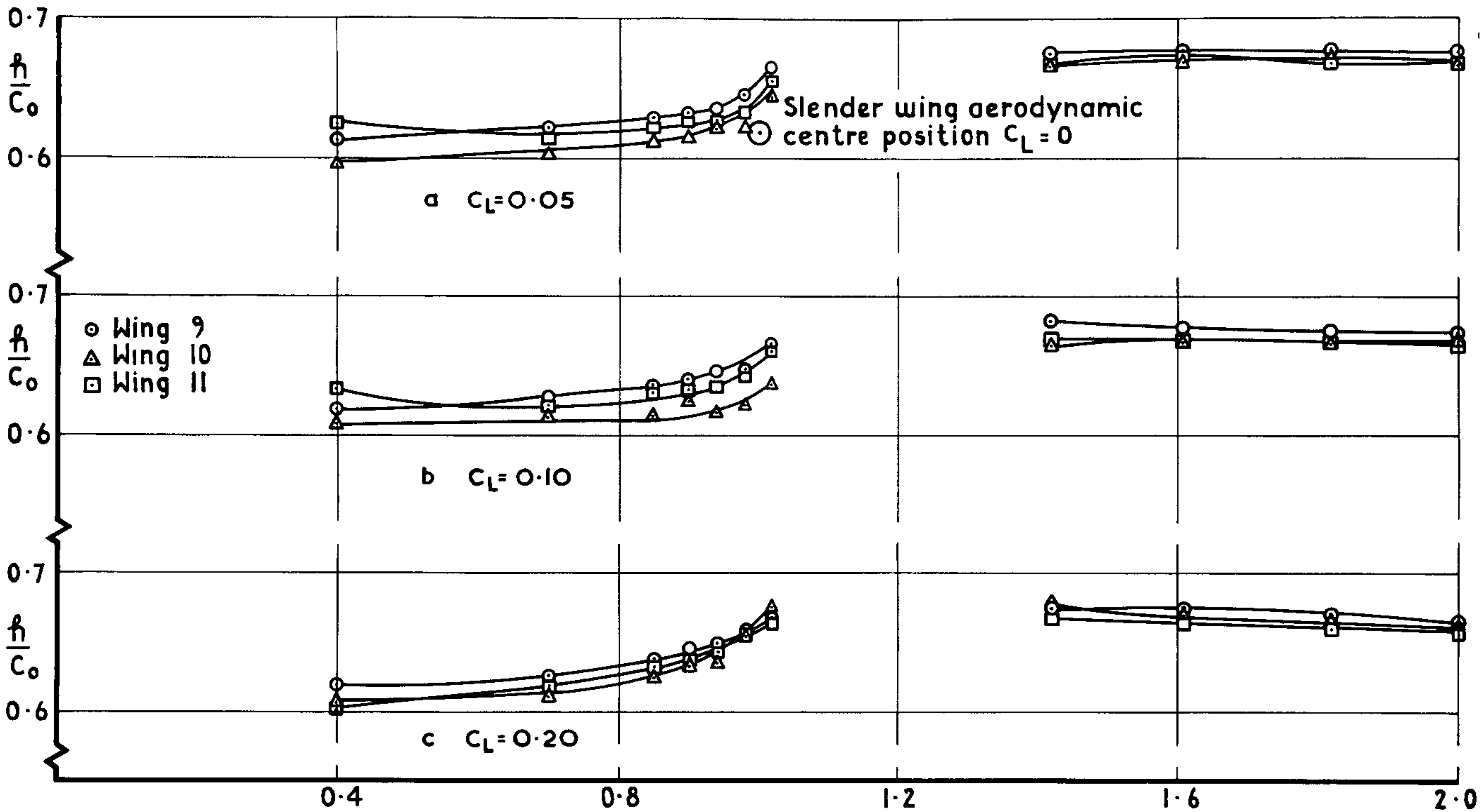

Fig.13 Variation of aerodynamic centre position with Mach Number and lift coefficient

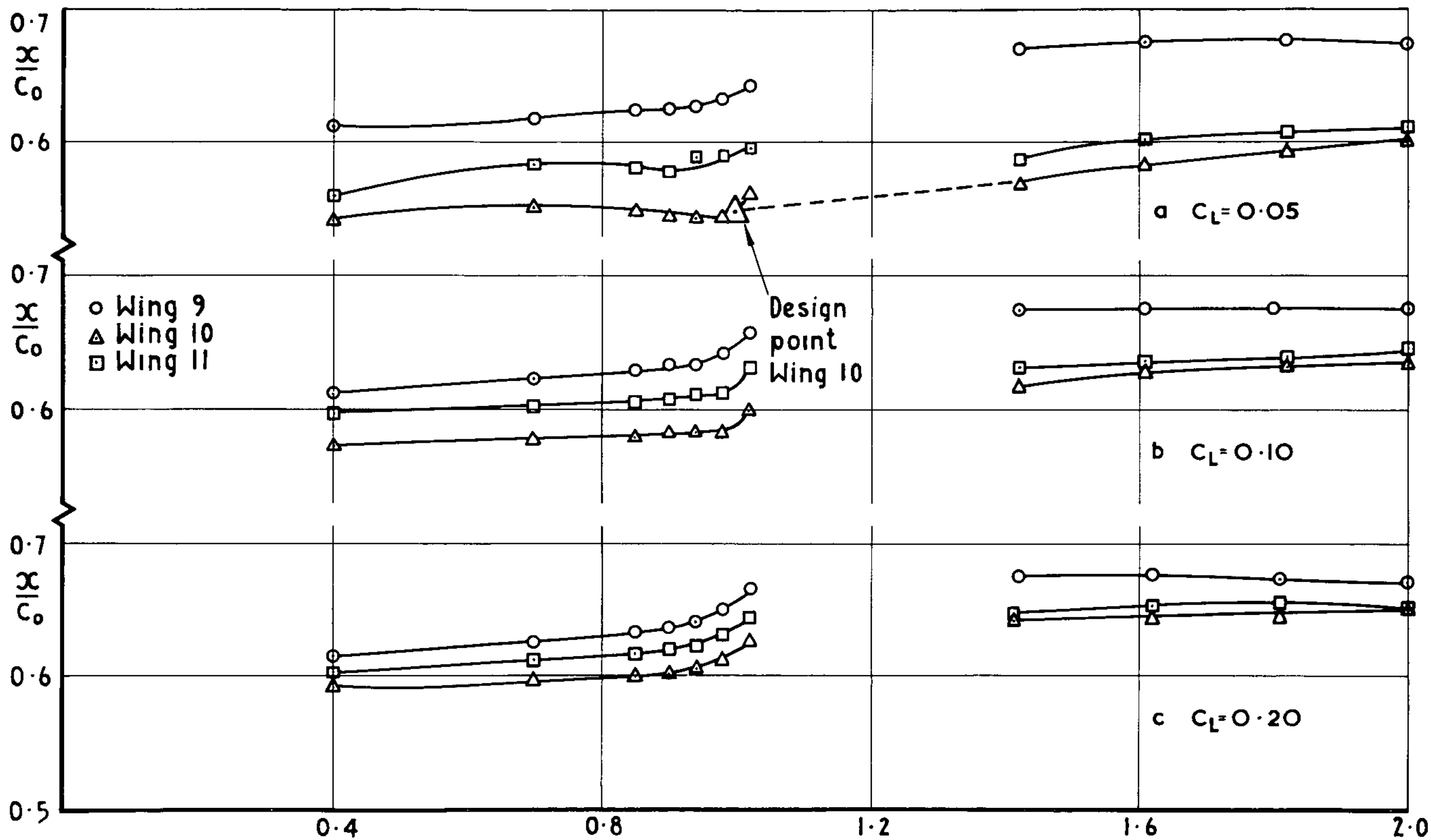

Fig. 14 Variation of centre of pressure position with Mach Number and lift coefficient

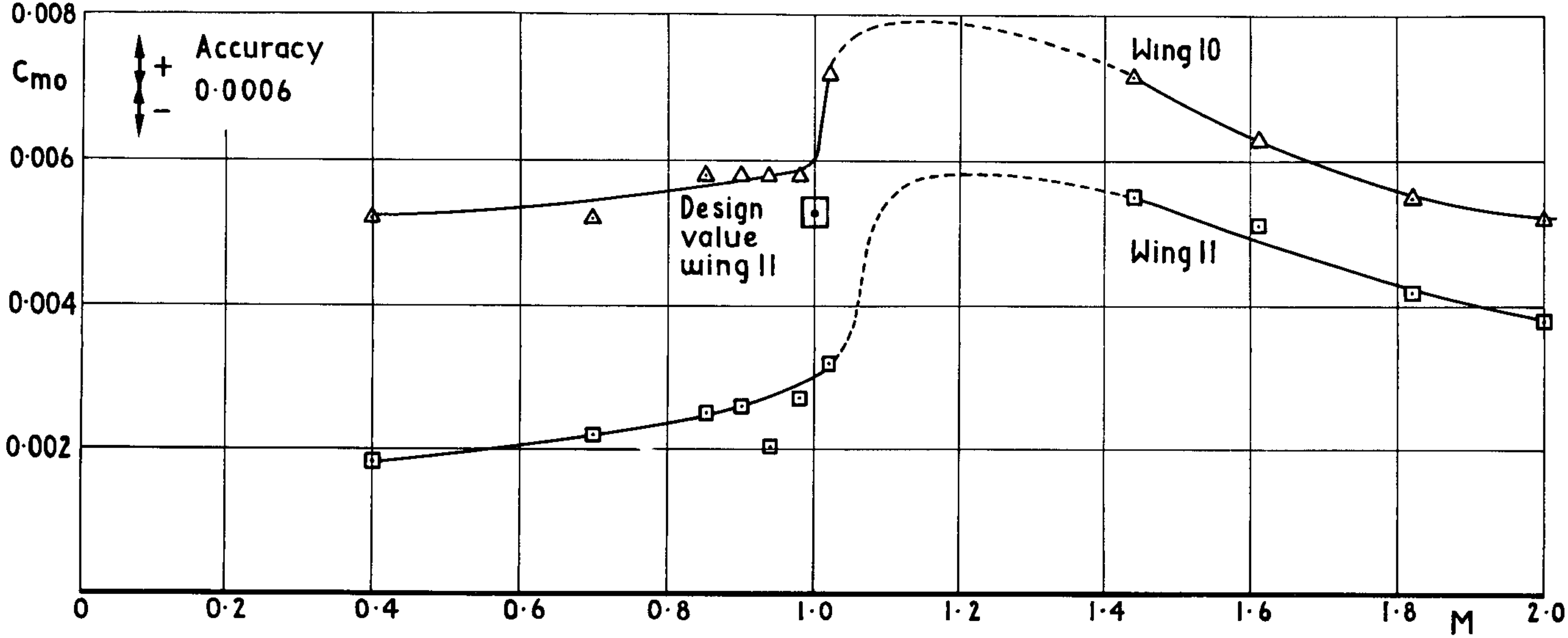

Fig.15 Wings 10 and 11. Variation of zero lift pitching moment with Mach Number

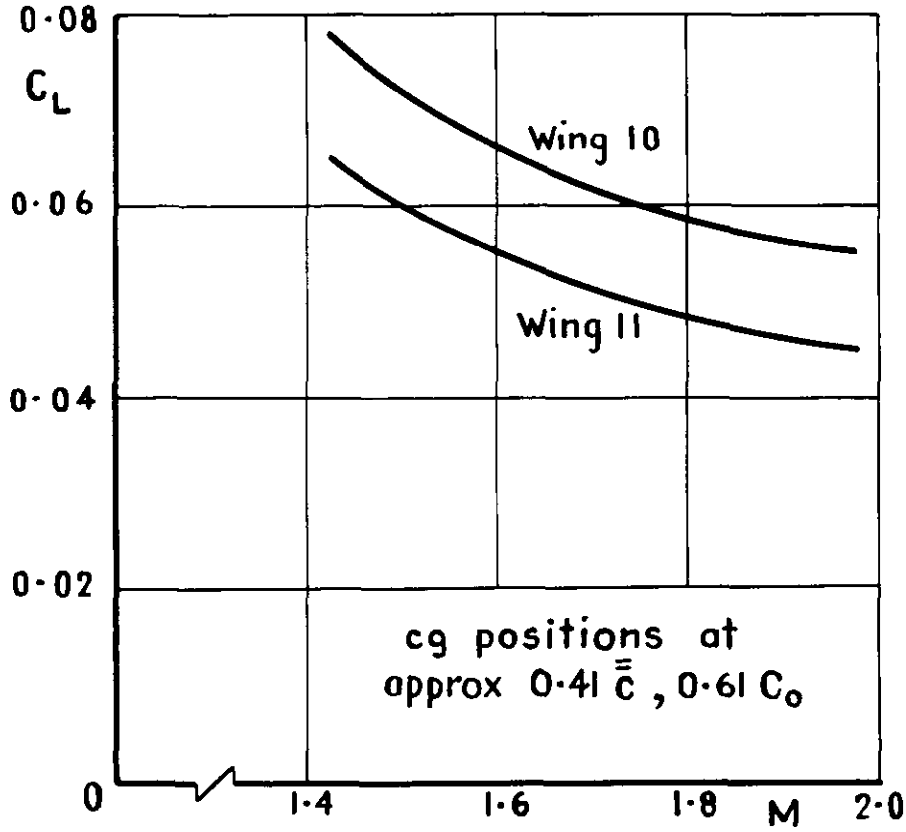

Fig. 16 Wing 10 and 11. Variation of trimmed lift coefficient with Mach No at supersonic speeds

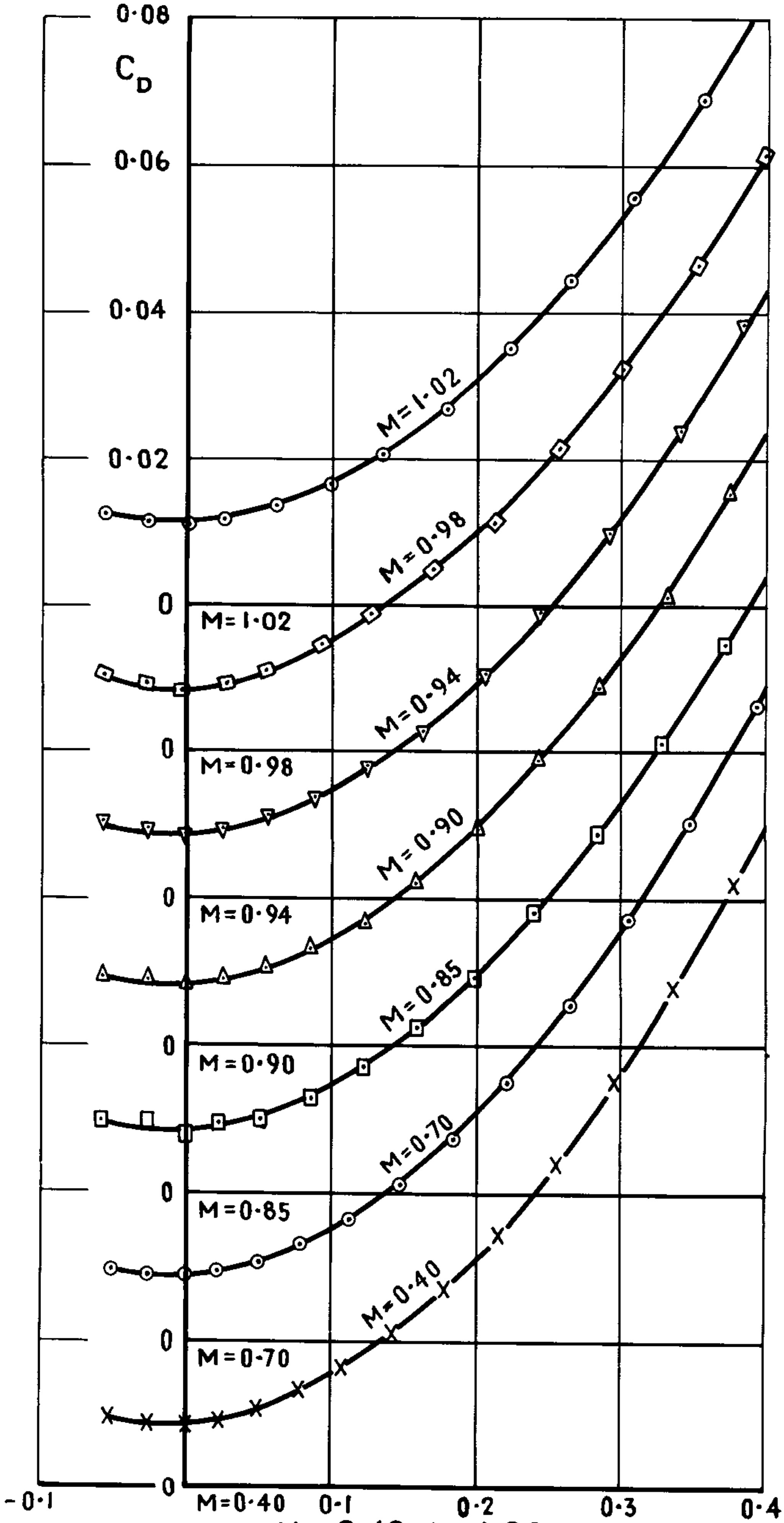

a M = 0·40 to 1·02

Fig. 17 Wing 9. Variation of drag coefficient with lift coefficient.

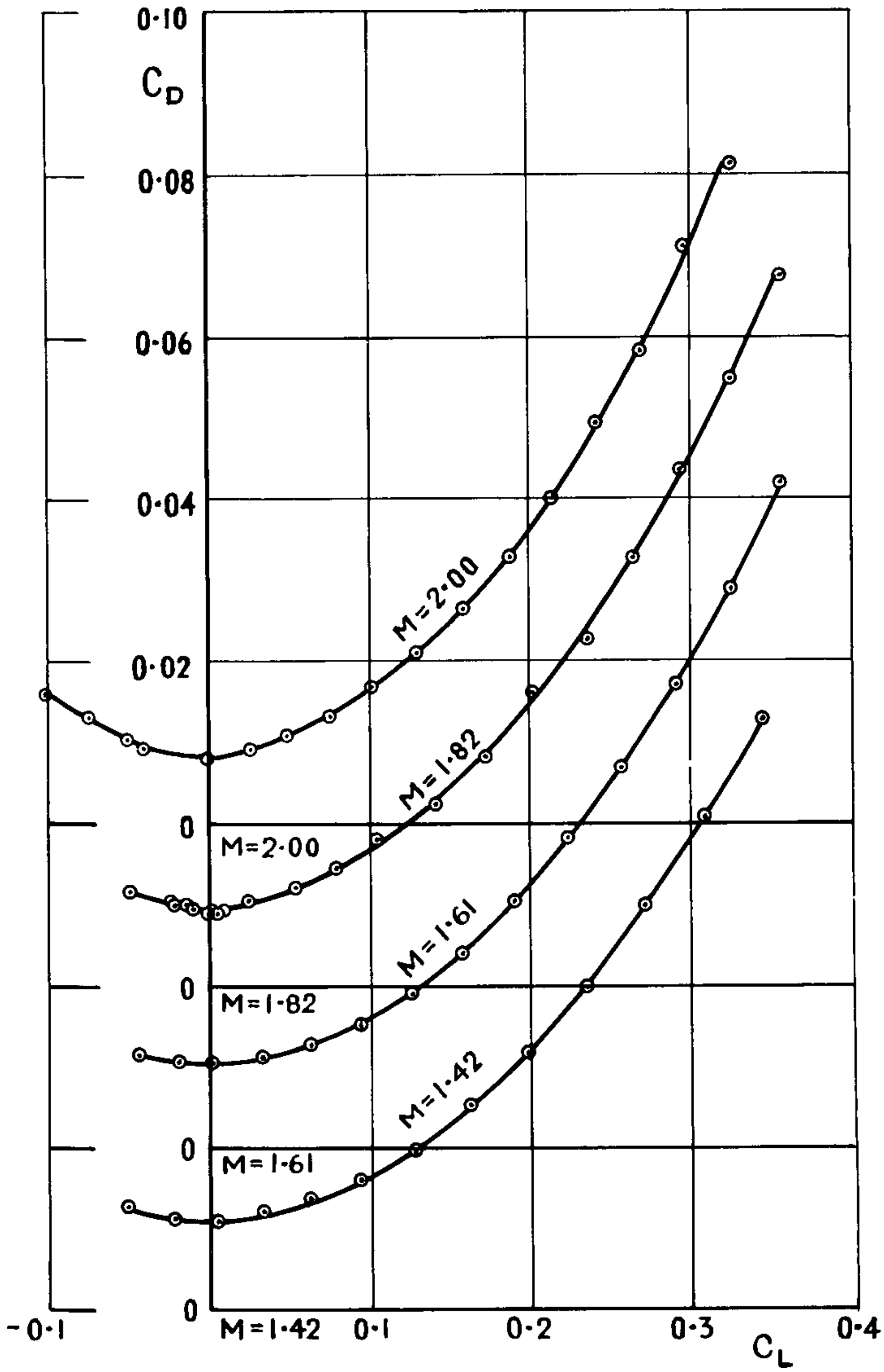

b M=1·42 to 2·00

Fig. 17 contd.

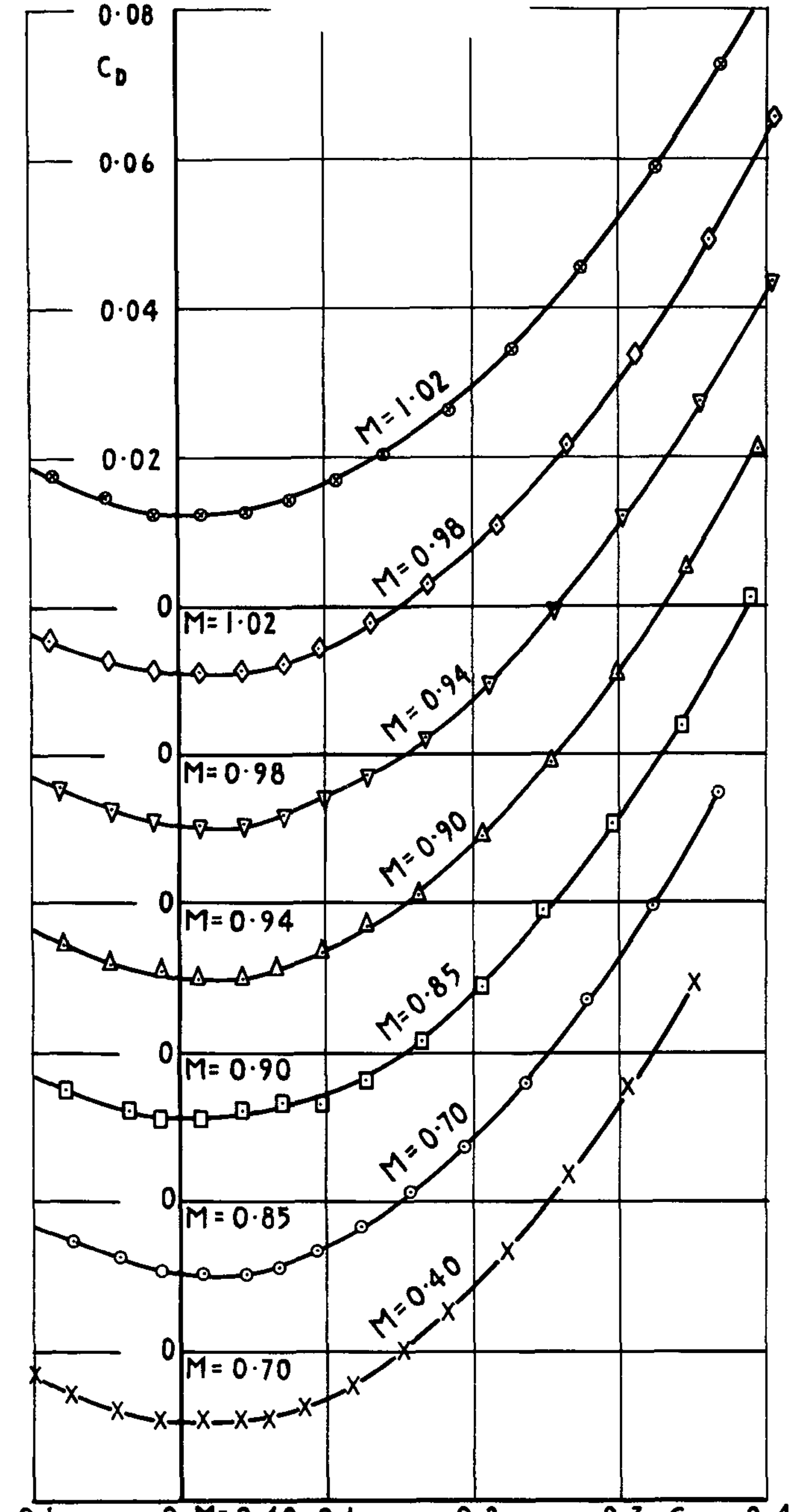

a M=0·40 to 1·02

Fig. 18 Wing 10. Variation of drag coefficient with lift coefficient

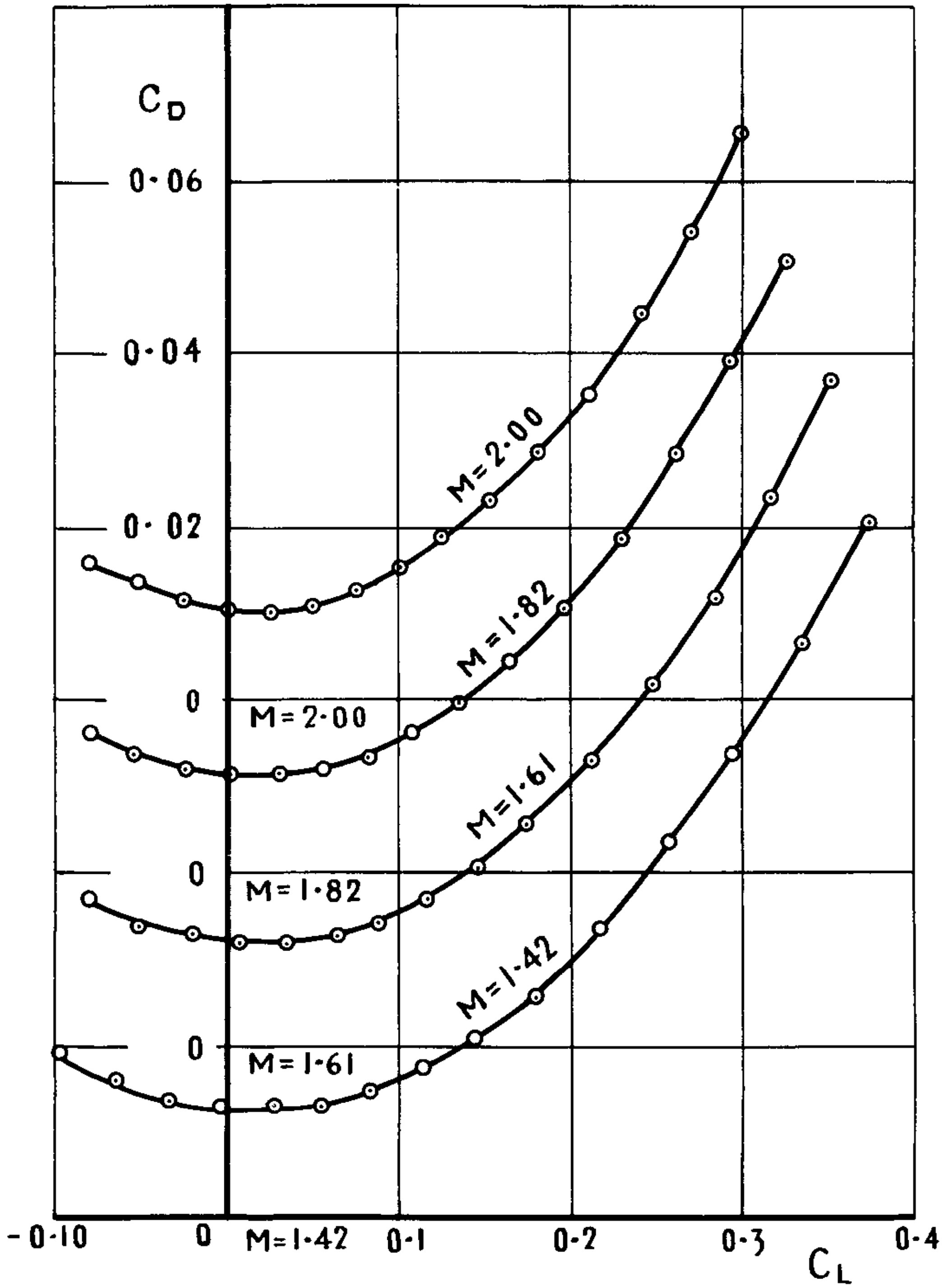
C_D
0·06
0·04
0·02
0
0
0
M=2·00
M=1·82
M=1·61
M=1·42
M=2·00
M=1·82
M=1·61
M=1·42
-0·10
0
0·1
0·2
0·3
0·4
C_L

b M=1·42 to 2·00

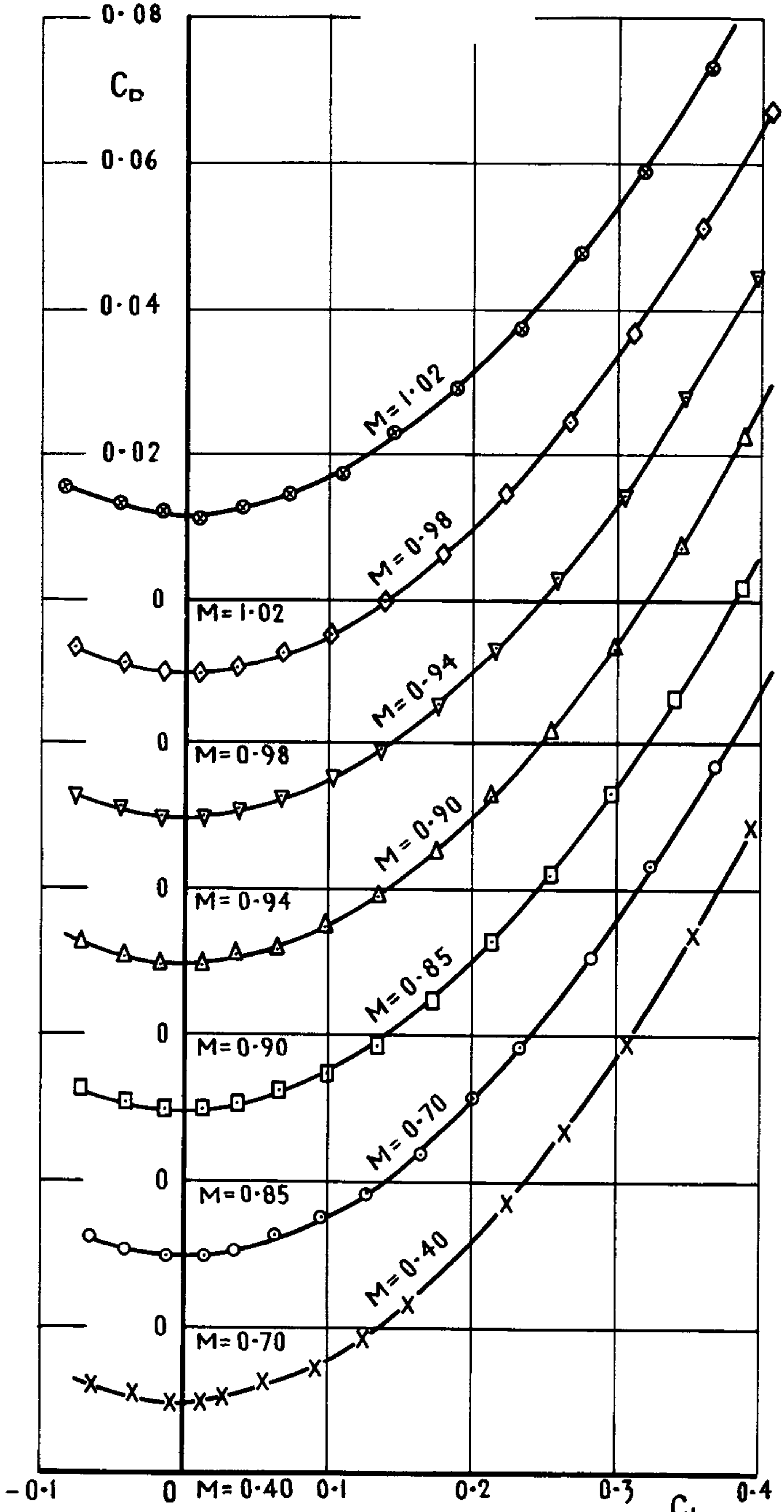

0·08
C_D
0·06
0·04
0·02
0
0
0
0
0
0
M=1·02
M=0·98
M=0·94
M=0·90
M=0·85
M=0·70
M=0·40
M=1·02
M=0·98
M=0·94
M=0·90
M=0·85
M=0·70
M=0·40
−0·1
0
0·1
0·2
0·3
0·4
C_L

a M=0·40 to 1·02

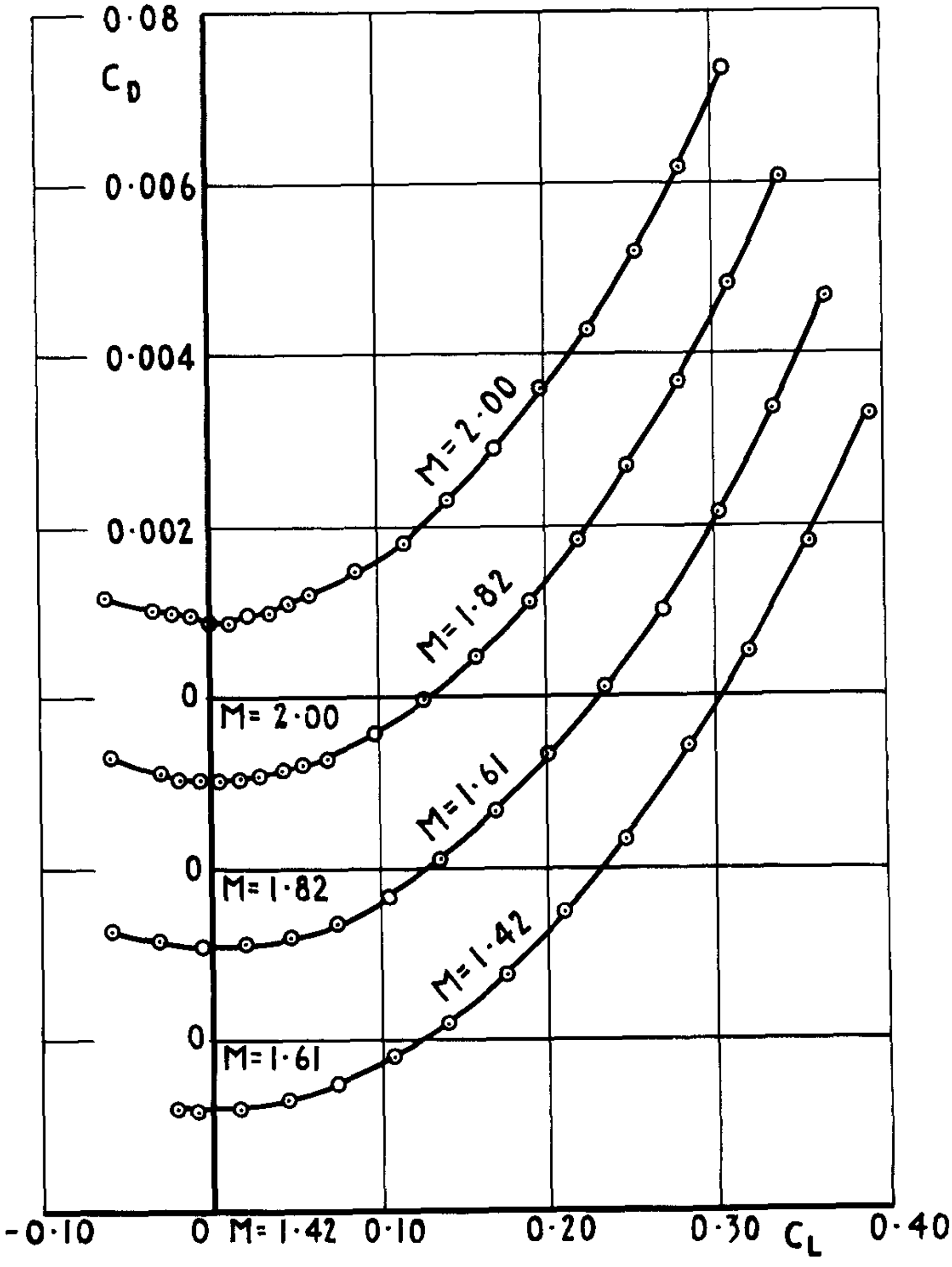

b M=1·42 to 2·00

Fig 19 contd.

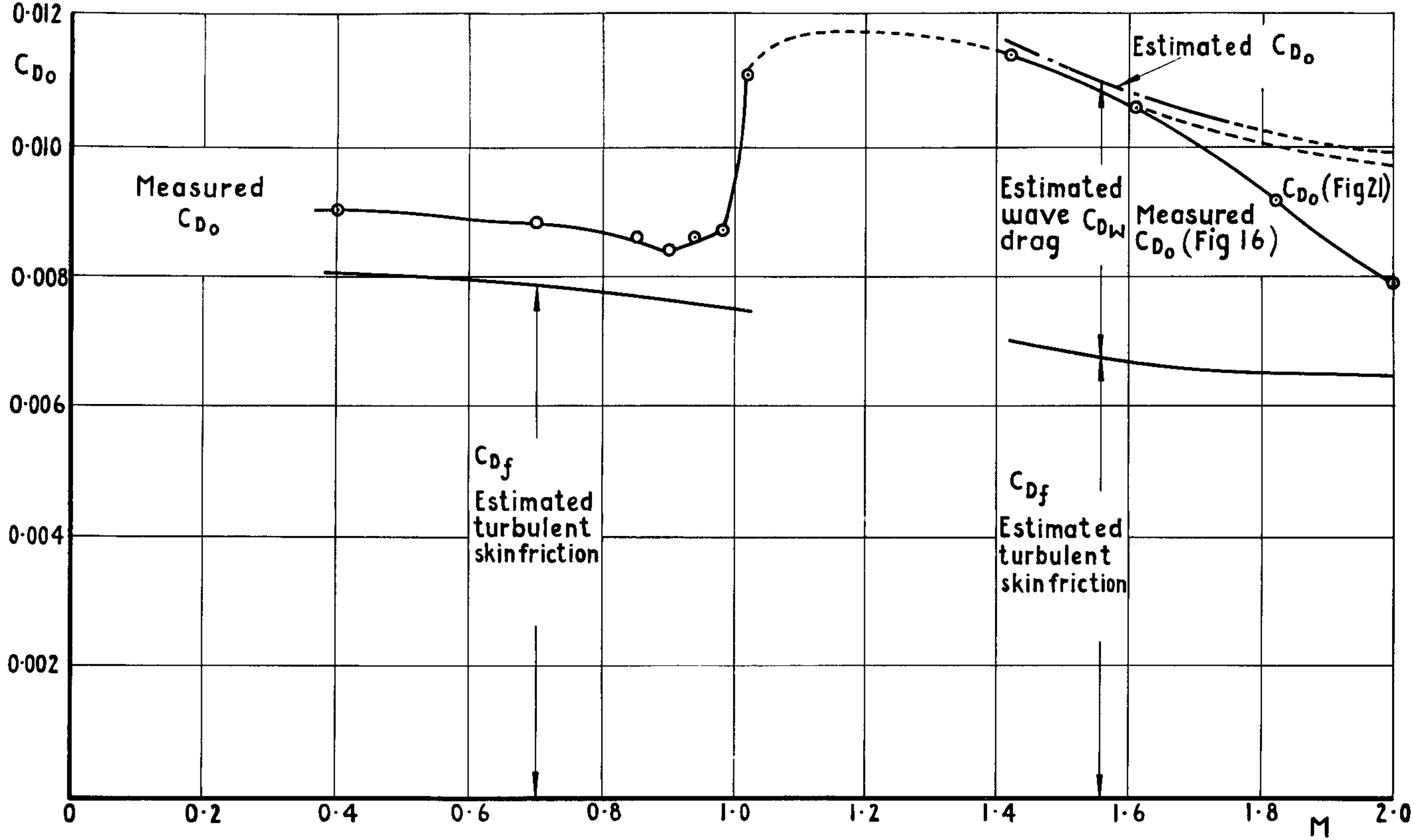

Fig. 20 Wing 9. Variation of C_{D_o} with Mach Number

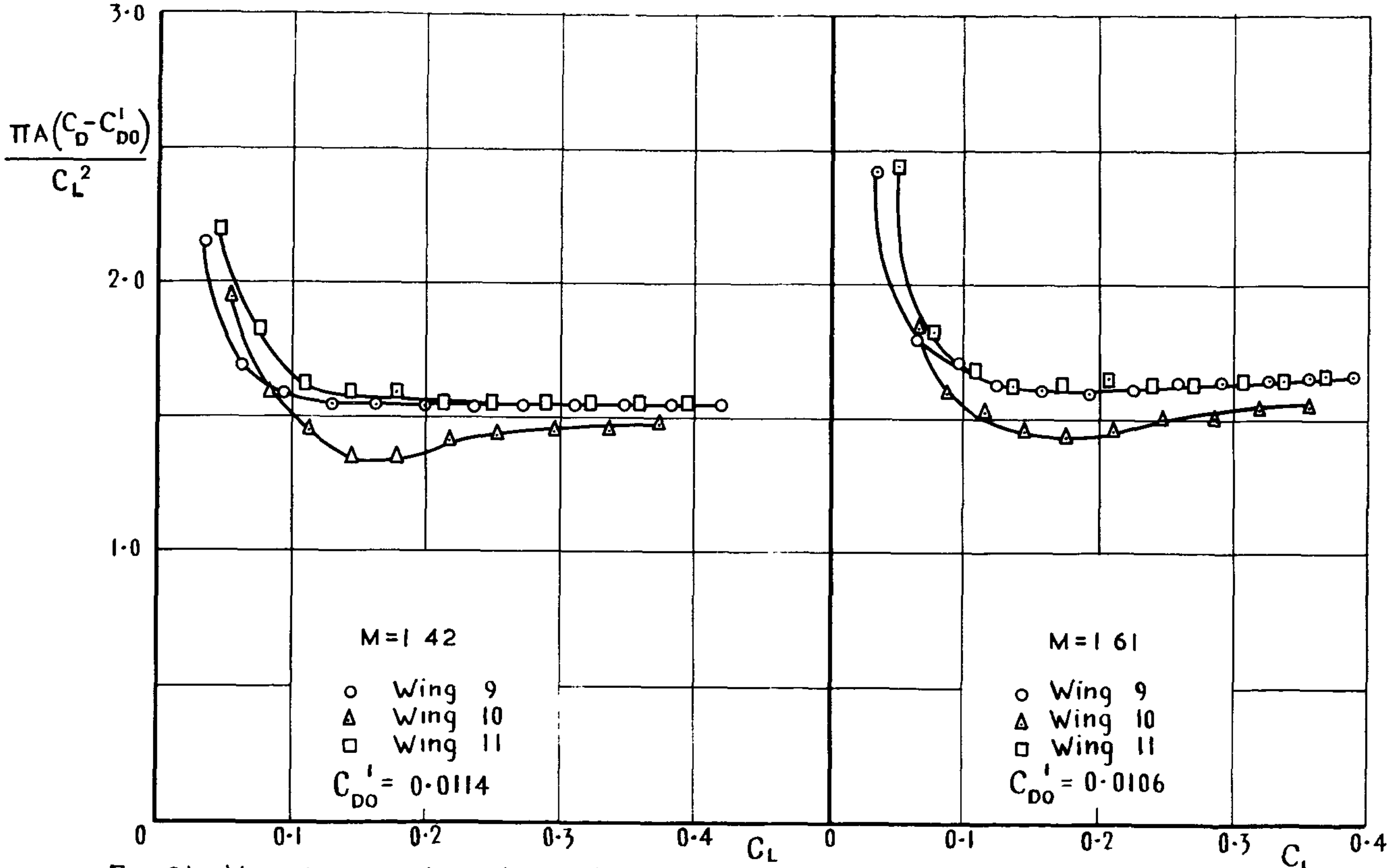

Fig 21 Variation of drag due to lift factor with lift coefficient and Mach number

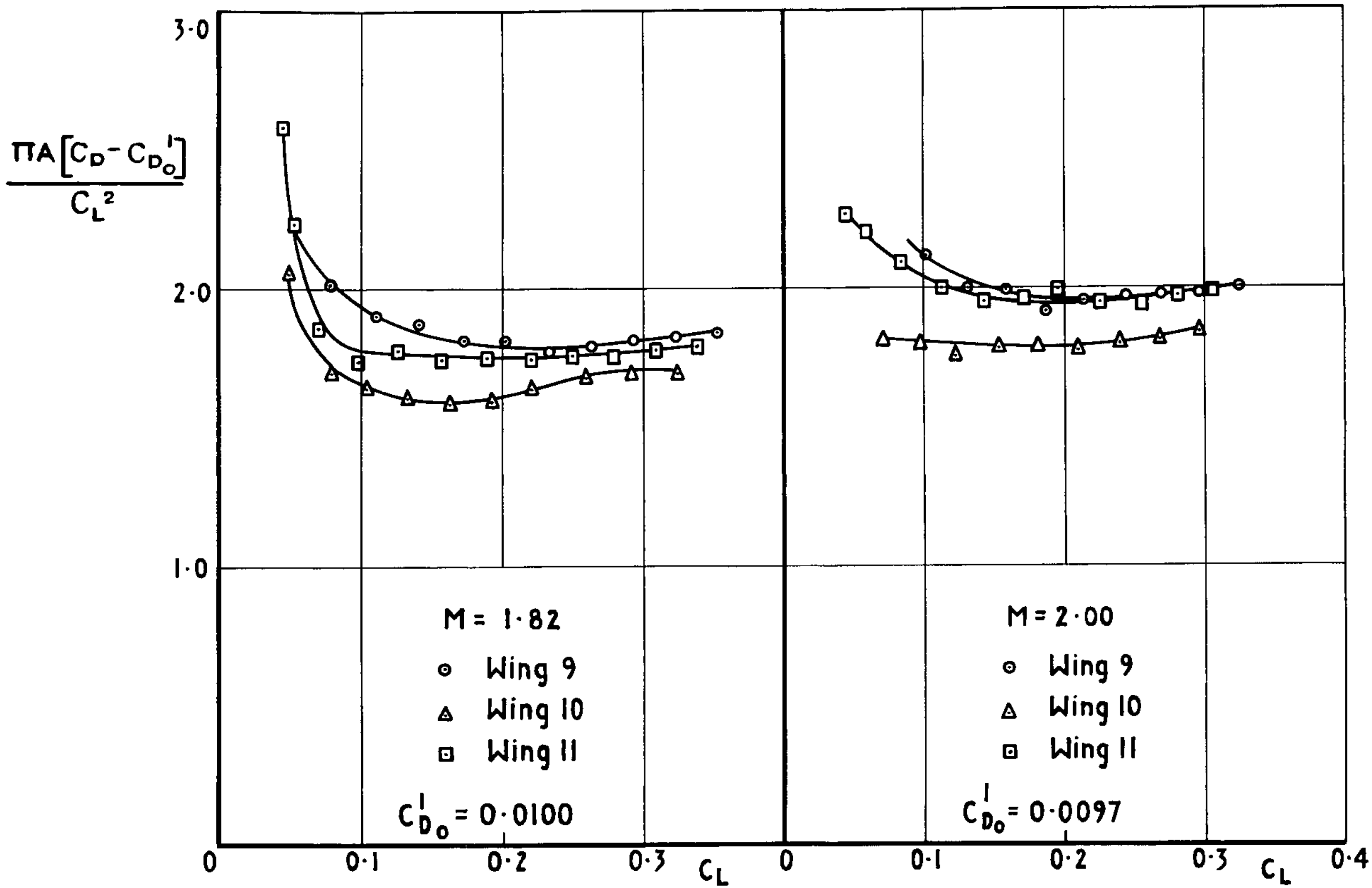
$\frac{\pi A\left[C_D - C_{D_0}'\right]}{C_L^2}$
3·0
2·0
1·0
0
0·1
0·2
0·3
0·4
C_L
M = 1·82
Wing 9
Wing 10
Wing 11
$C_{D_0}' = 0·0100$
M = 2·00
Wing 9
Wing 10
Wing 11
$C_{D_0}' = 0·0097$

Fig 21 contd

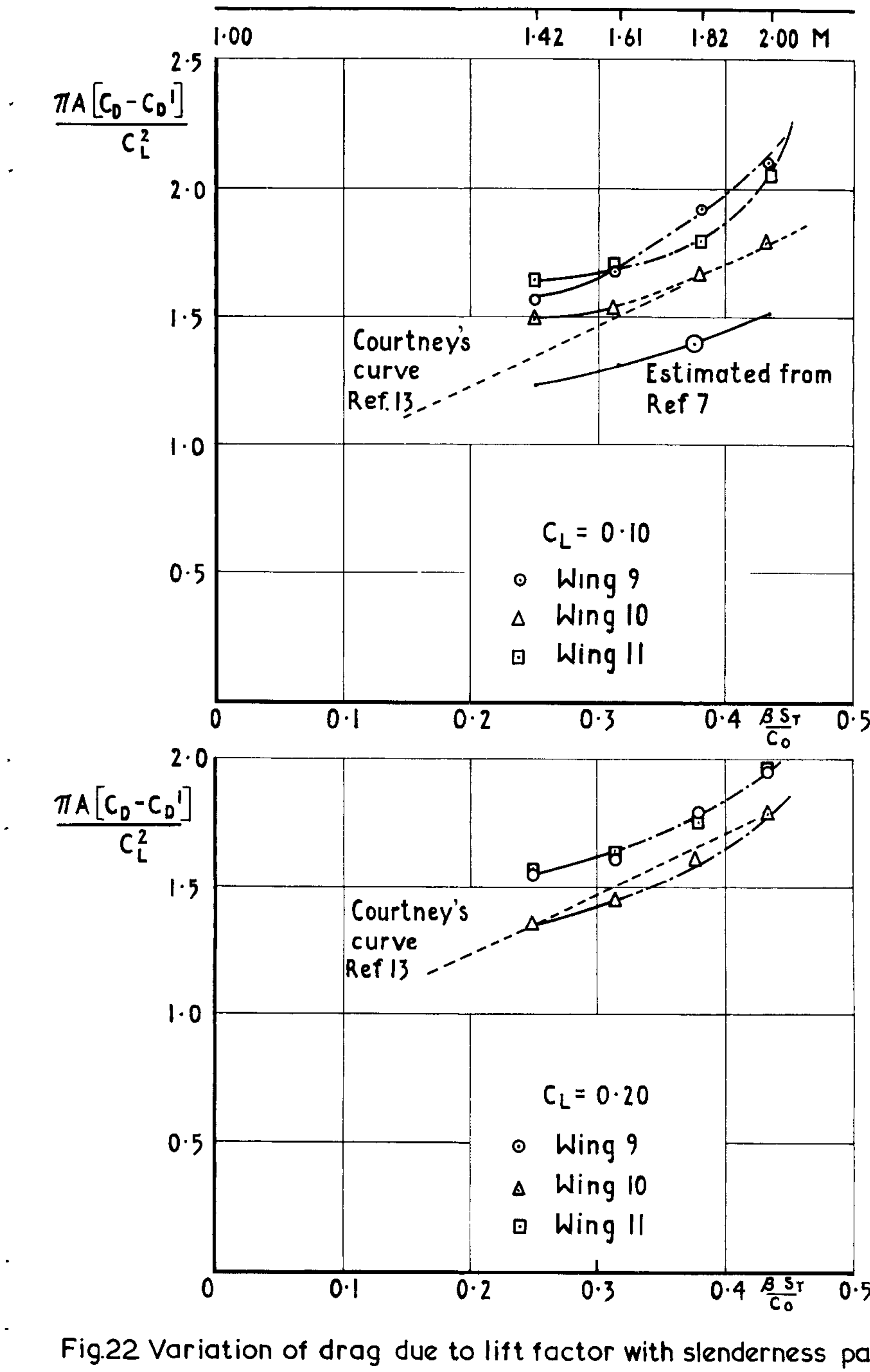

Fig.22 Variation of drag due to lift factor with slenderness parameter

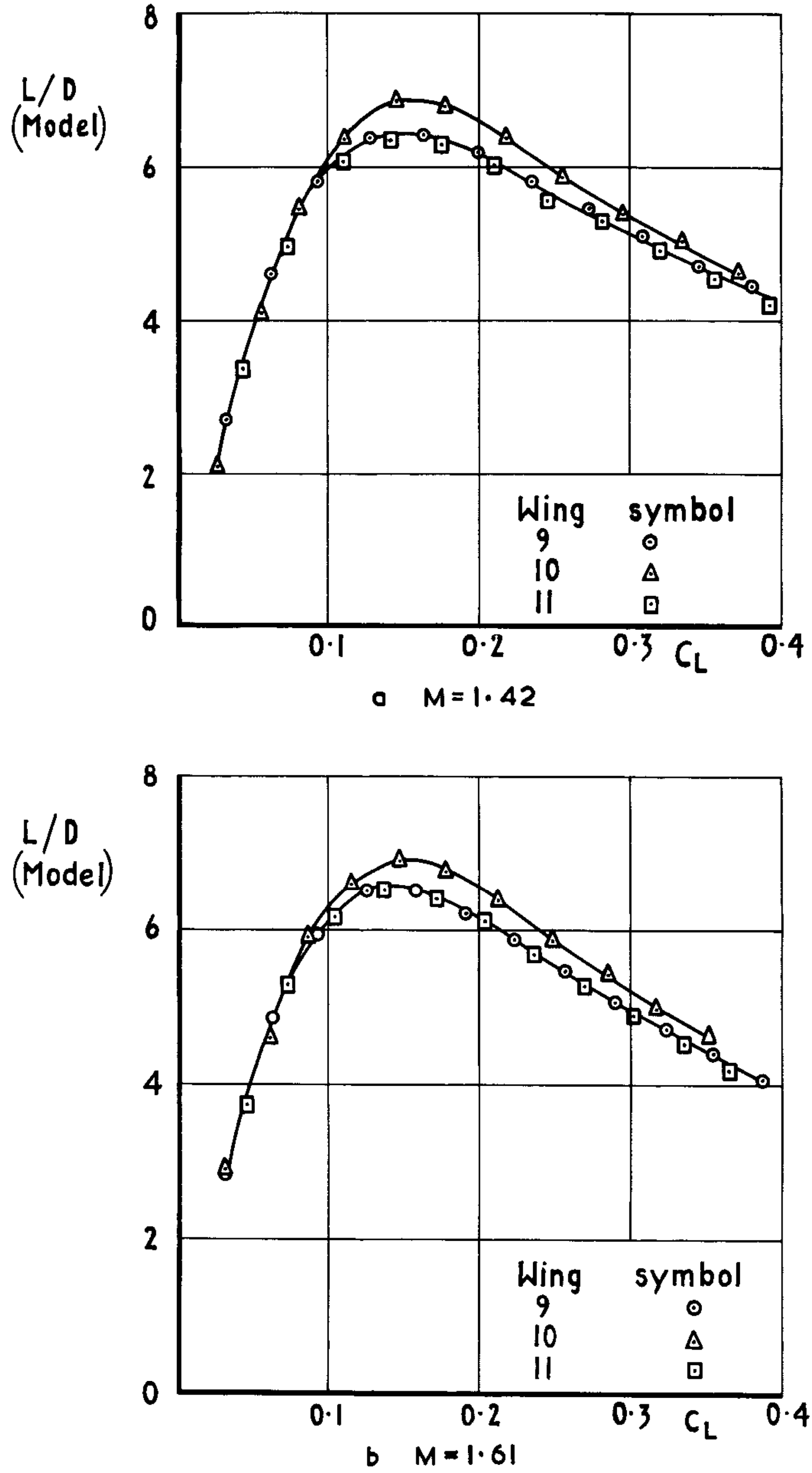

Fig 23 Variation of lift/drag ratio with lift coefficient

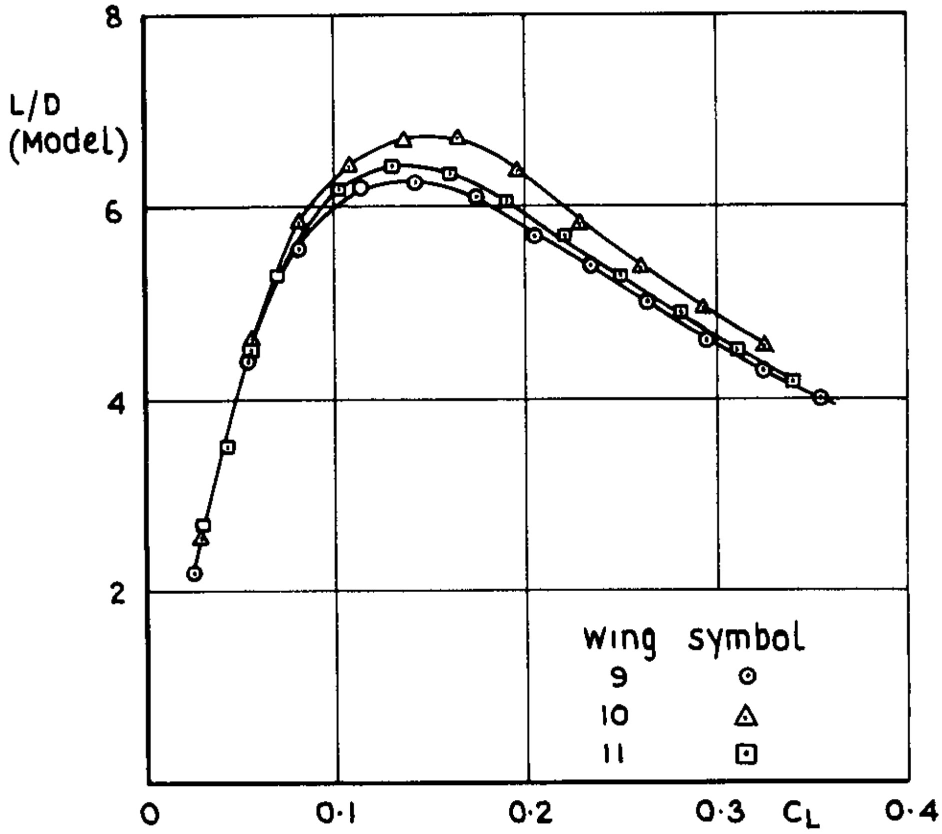

c M= 1·82

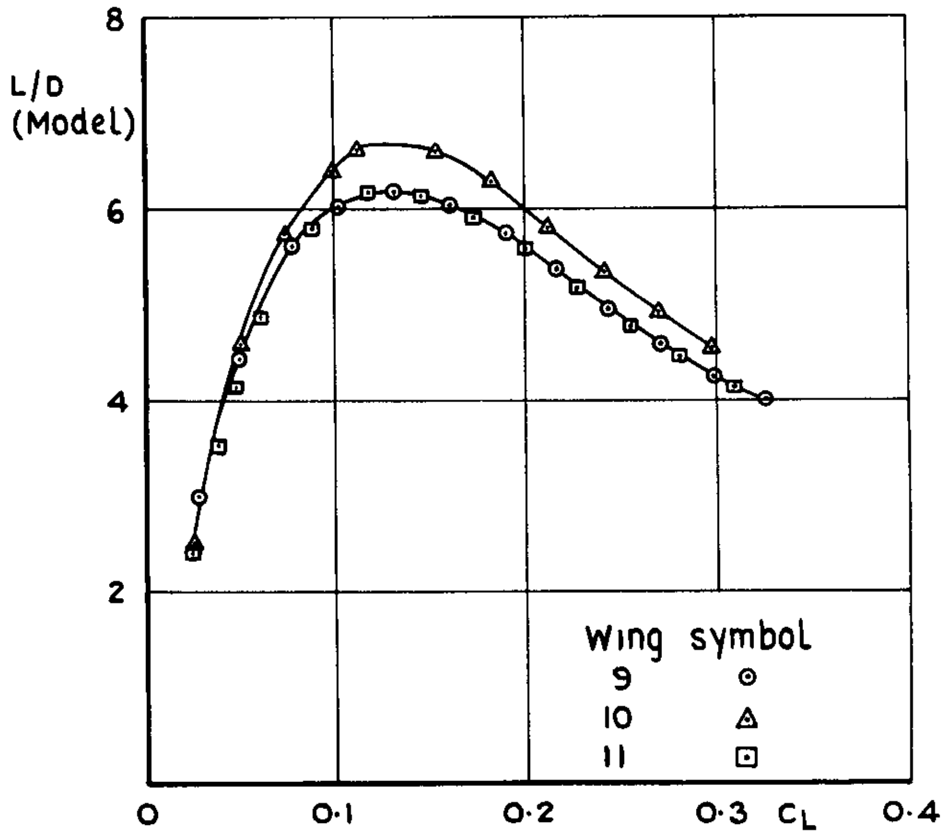

d M= 2·00

Fig. 23 contd

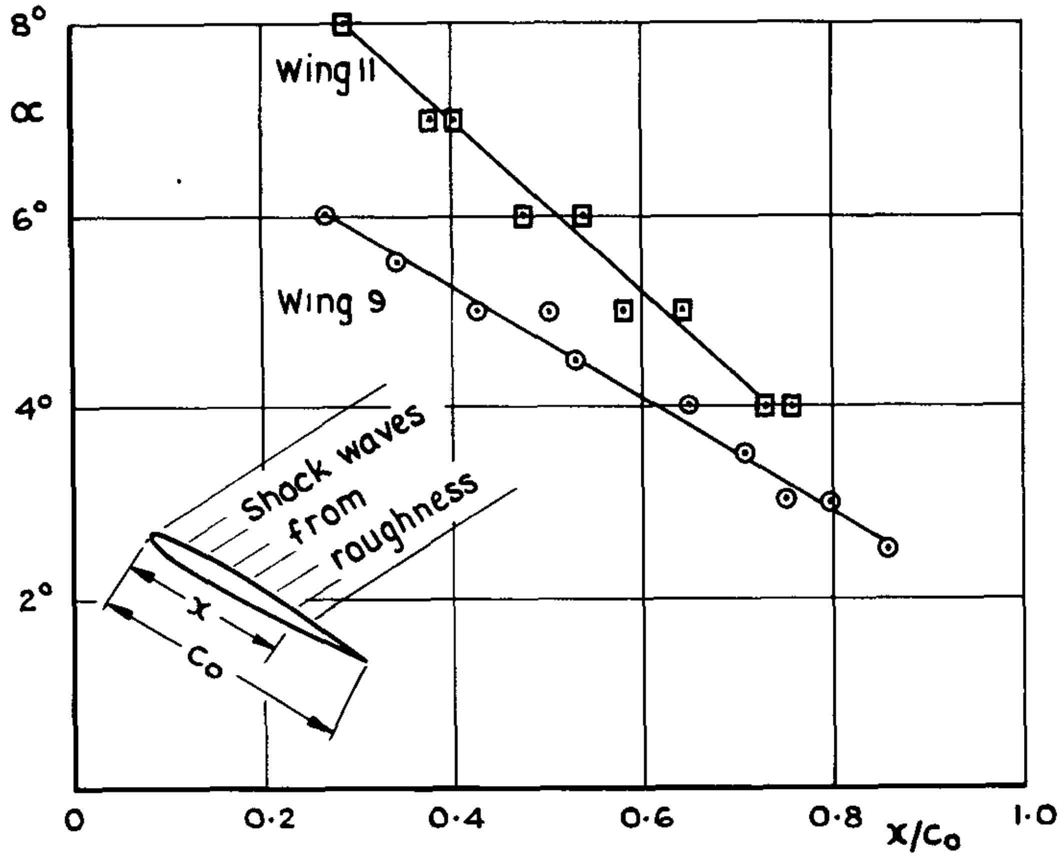

Fig. 24 Variation of roughness shock wave positions with incidence M=2·0 carborundum 0·020 in high.

Printed in England for Her Majesty's Stationery Office by the Royal Aircraft Establishment, Farnborough. Dd.135645. K.3.

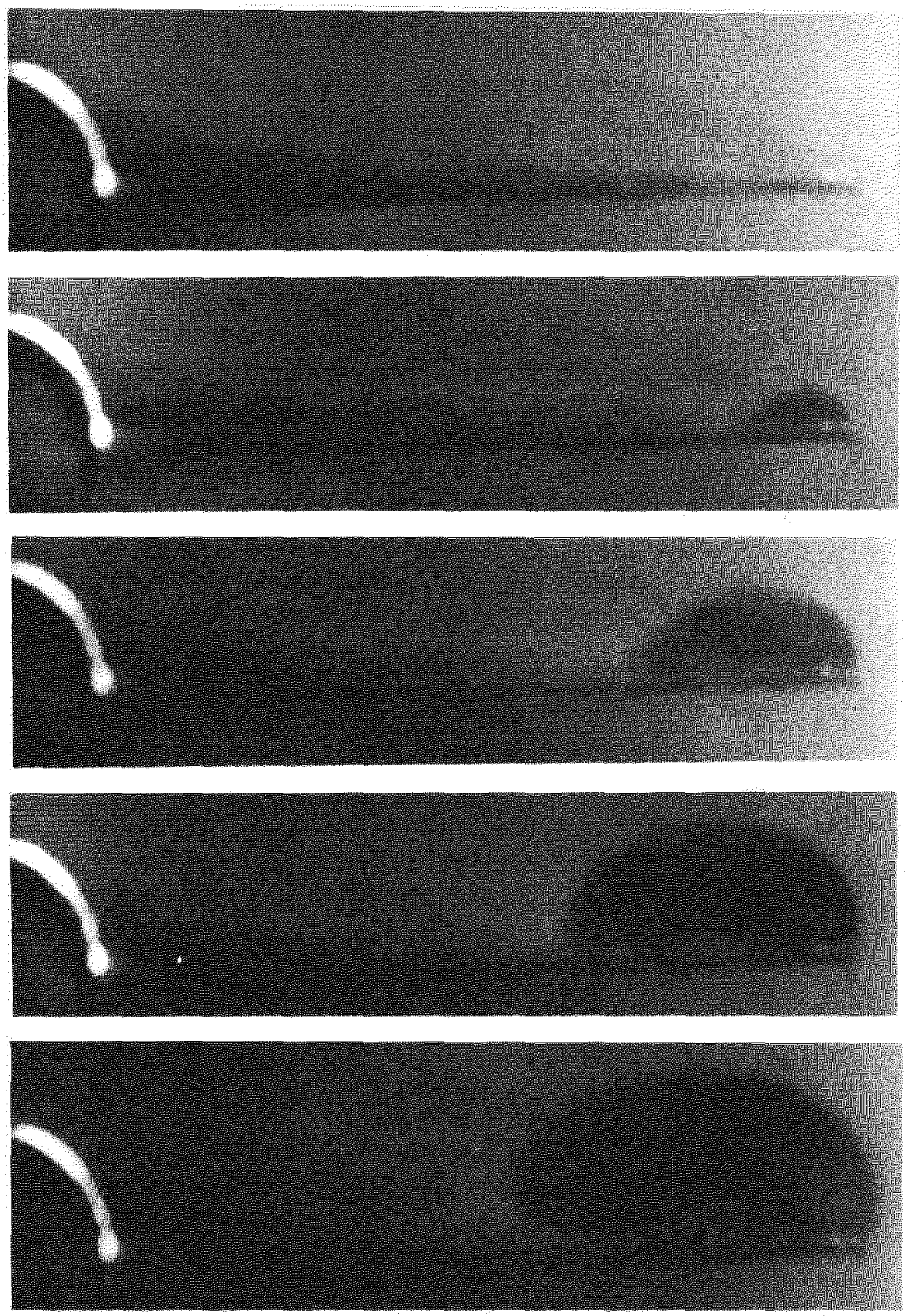

$\alpha = 0°$
$\alpha - \bar{\alpha} = 0°$

$\alpha = 2.1°$
$\alpha - \bar{\alpha} = 2.1°$

$\alpha = 4.1°$
$\alpha - \bar{\alpha} = 4.1°$

$\alpha = 6.2°$
$\alpha - \bar{\alpha} = 6.2°$

$\alpha = 8.3°$
$\alpha - \bar{\alpha} = 8.3°$

(a) WING 9

Fig.25 Vapour screen photographs at the trailing-edge $M = 1{\cdot}8$

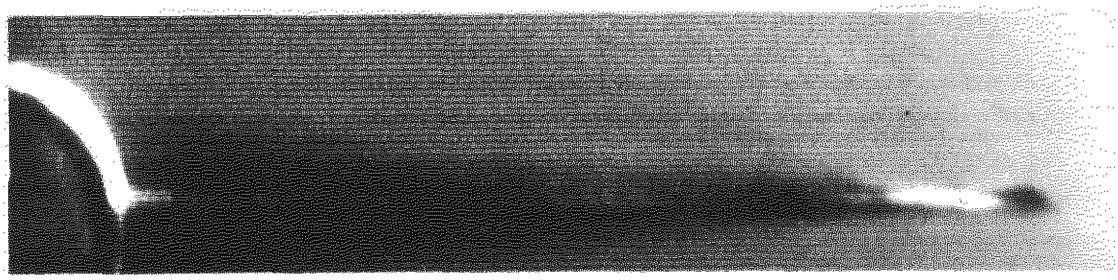

$\alpha = 4.1°$
$\alpha - \bar{\alpha} = 0.1°$

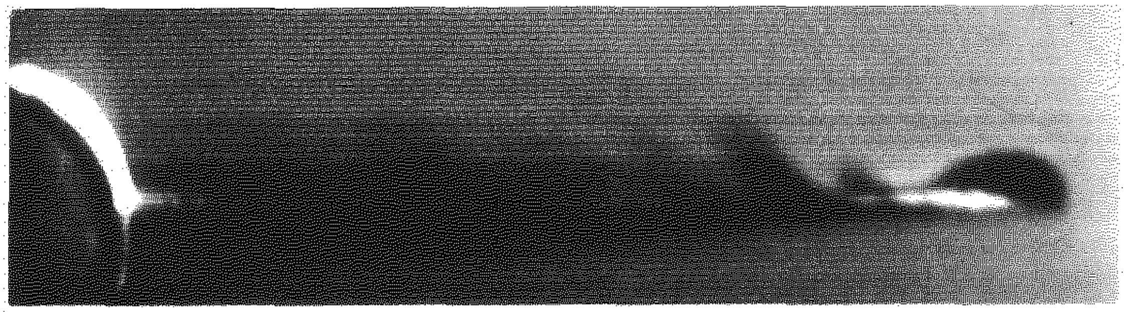

$\alpha = 6.2°$
$\alpha - \bar{\alpha} = 2.1°$

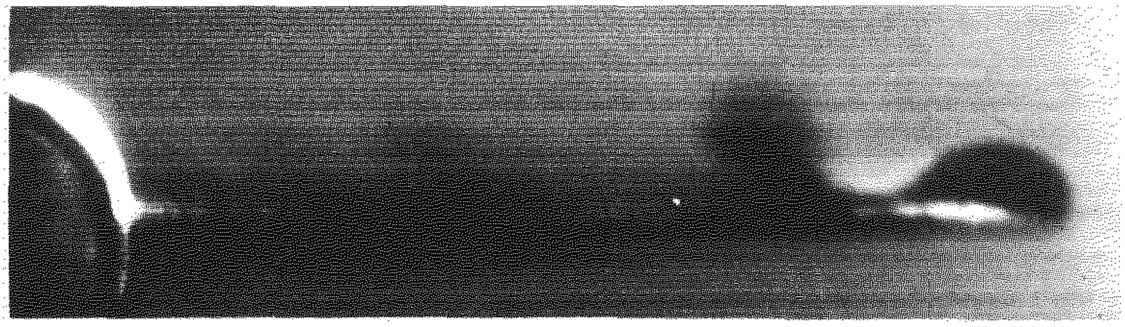

$\alpha = 7.3°$
$\alpha - \bar{\alpha} = 3.2°$

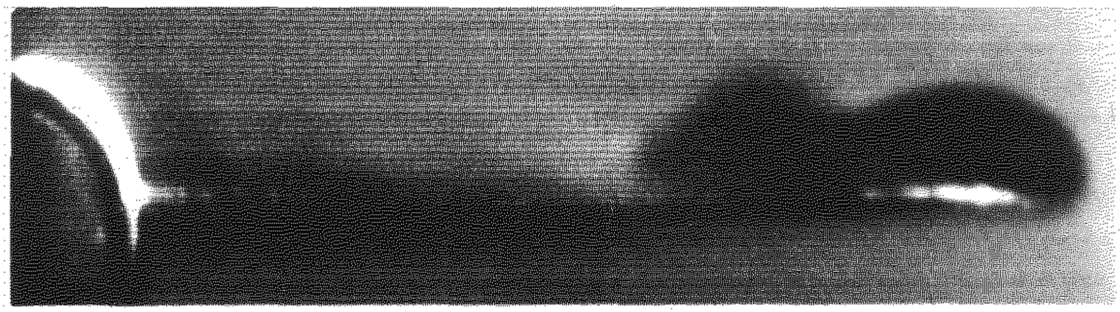

$\alpha = 8.3°$
$\alpha - \bar{\alpha} = 4.2°$

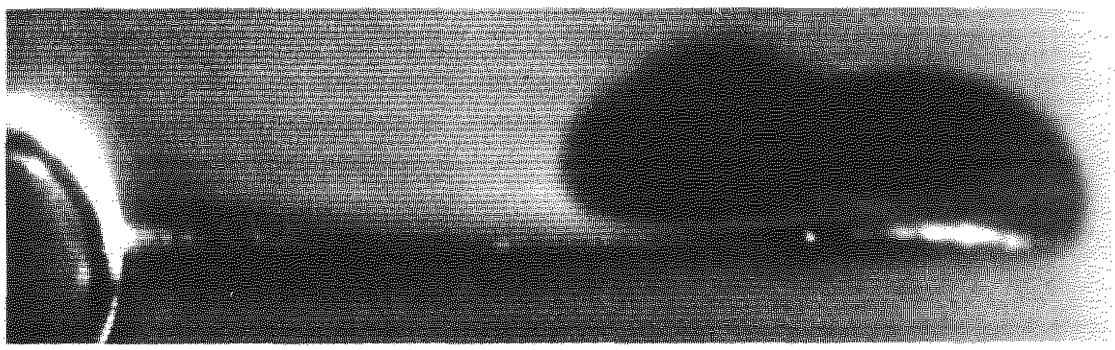

$\alpha = 10.4°$
$\alpha - \bar{\alpha} = 6.2°$

(b) WING 10

Fig.25 Continued

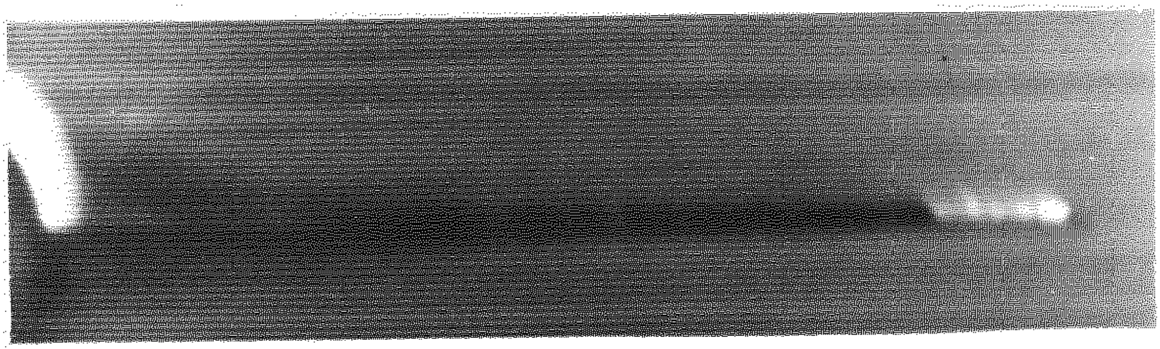

$\alpha = 0°$
$\alpha - \bar{\alpha} = -1°$

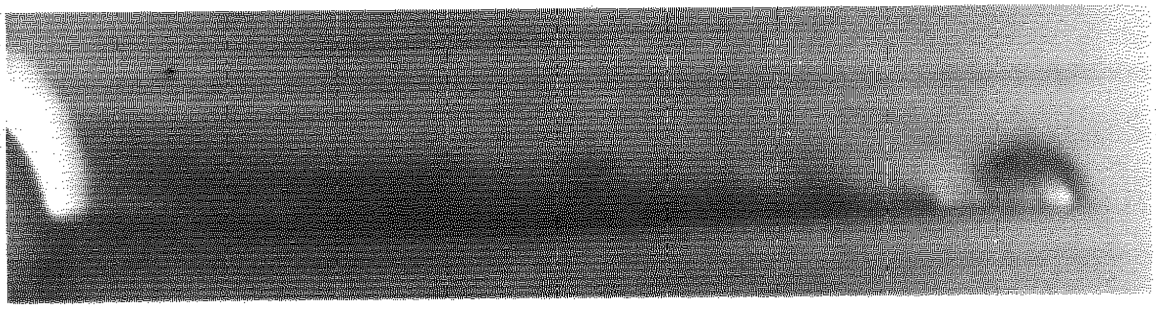

$\alpha = 2.1°$
$\alpha - \bar{\alpha} = 1.1°$

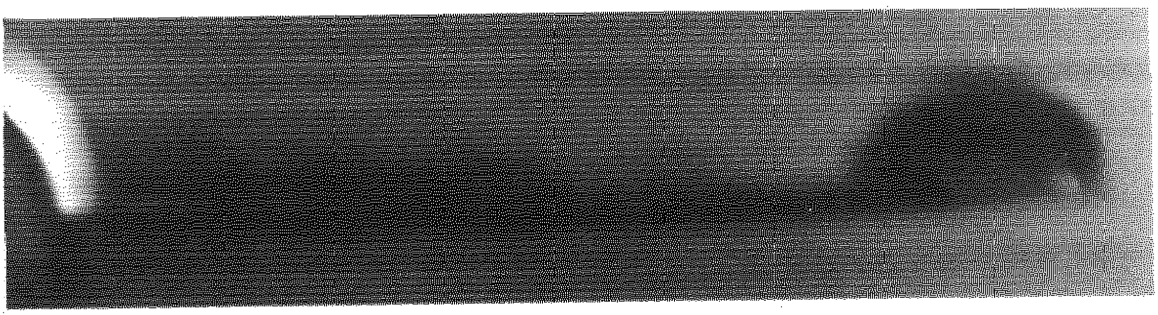

$\alpha = 4.2°$
$\alpha - \bar{\alpha} = 3.2°$

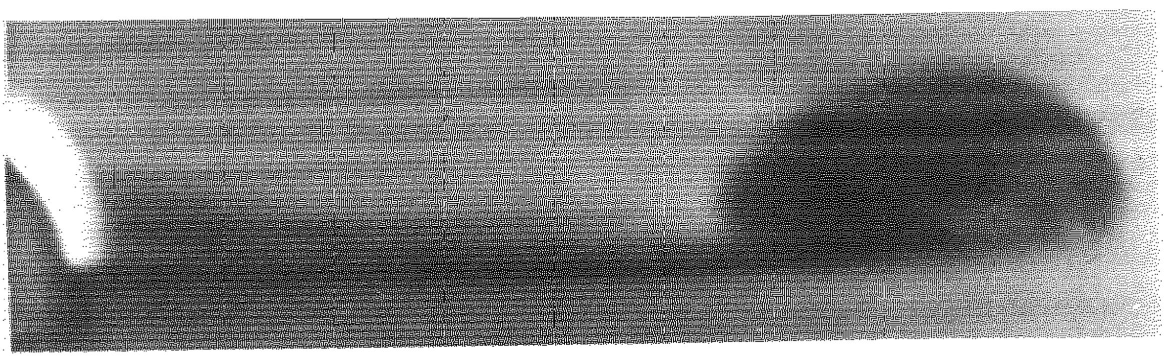

$\alpha = 6.2°$
$\alpha - \bar{\alpha} = 5.2°$

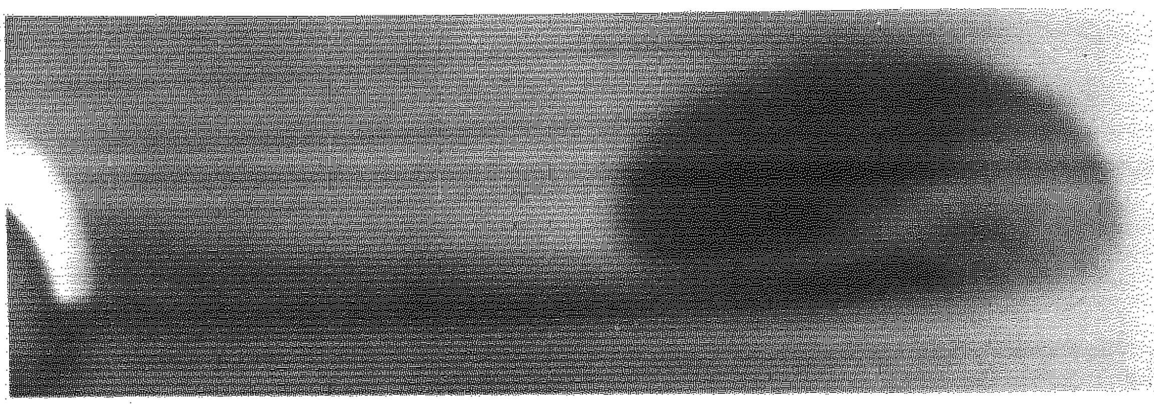

$\alpha = 8.3°$
$\alpha - \bar{\alpha} = 7.3°$

(c) WING 11

Fig.25 Concluded

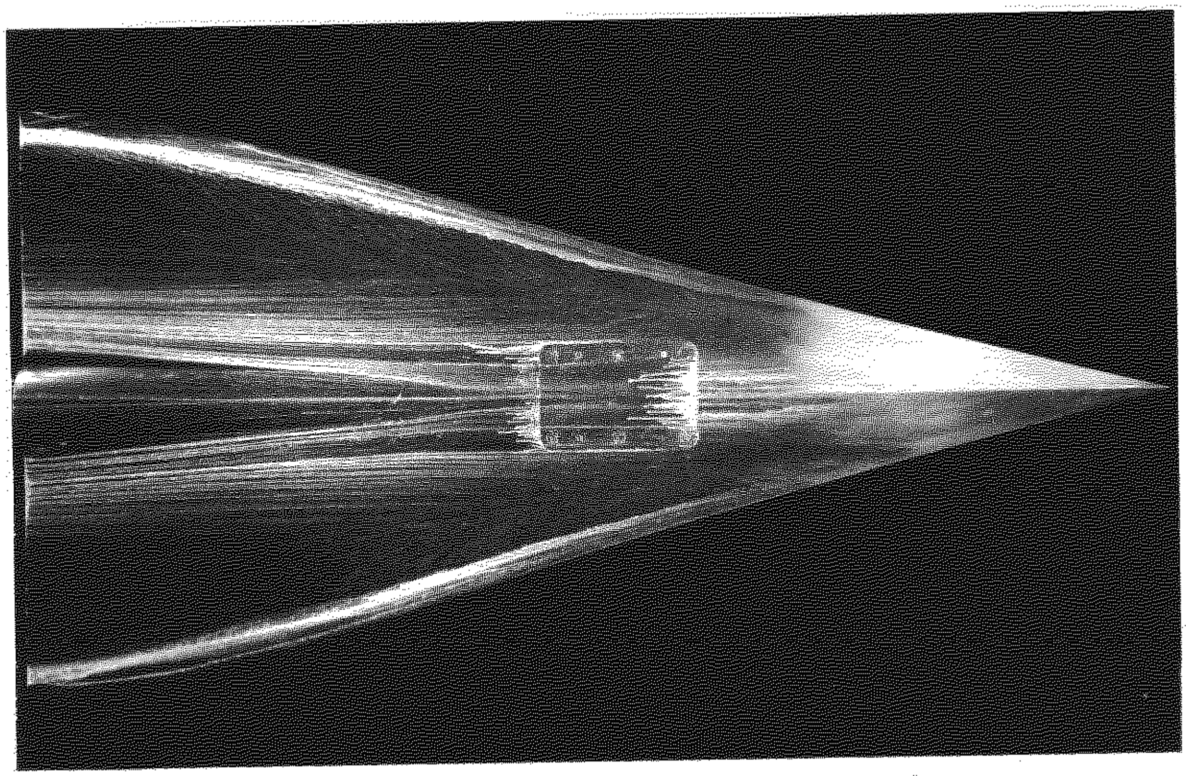

(a) M = 2.0 α = 5.1° (NO ROUGHNESS)

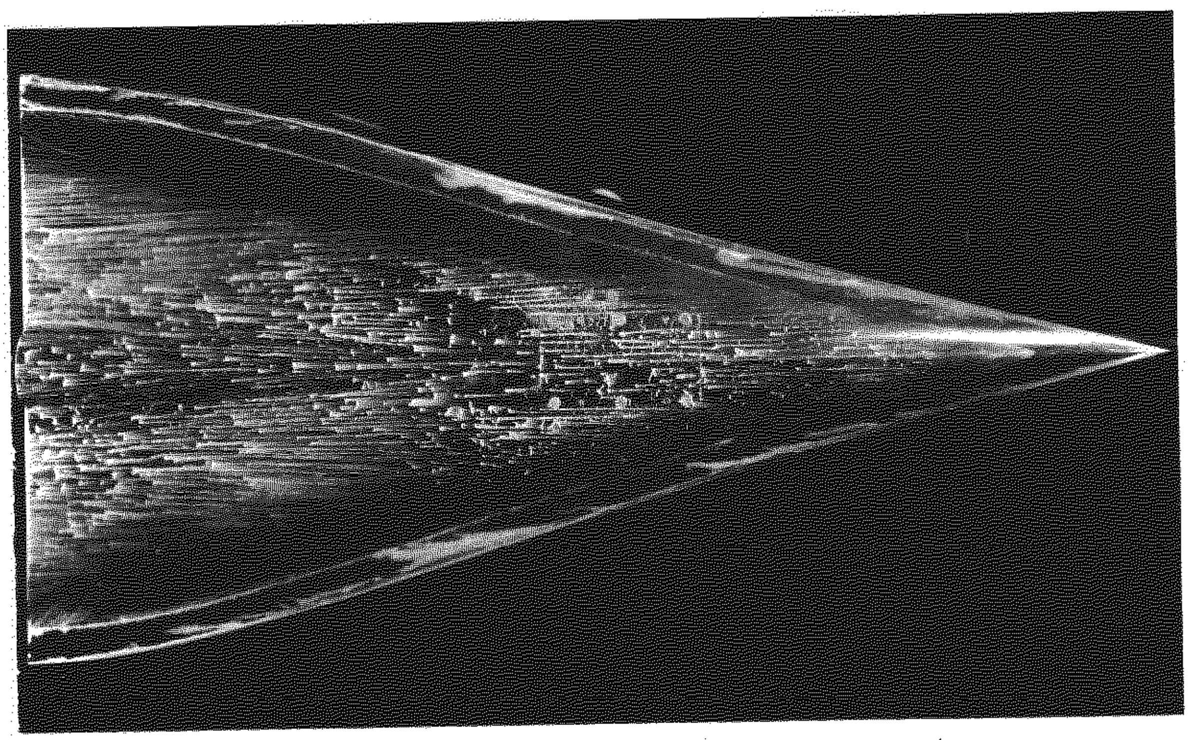

(b) M = 0.40 α = 5.1° (ROUGHNESS BAND)

Fig.26 Wing 9. Oil flow photographs

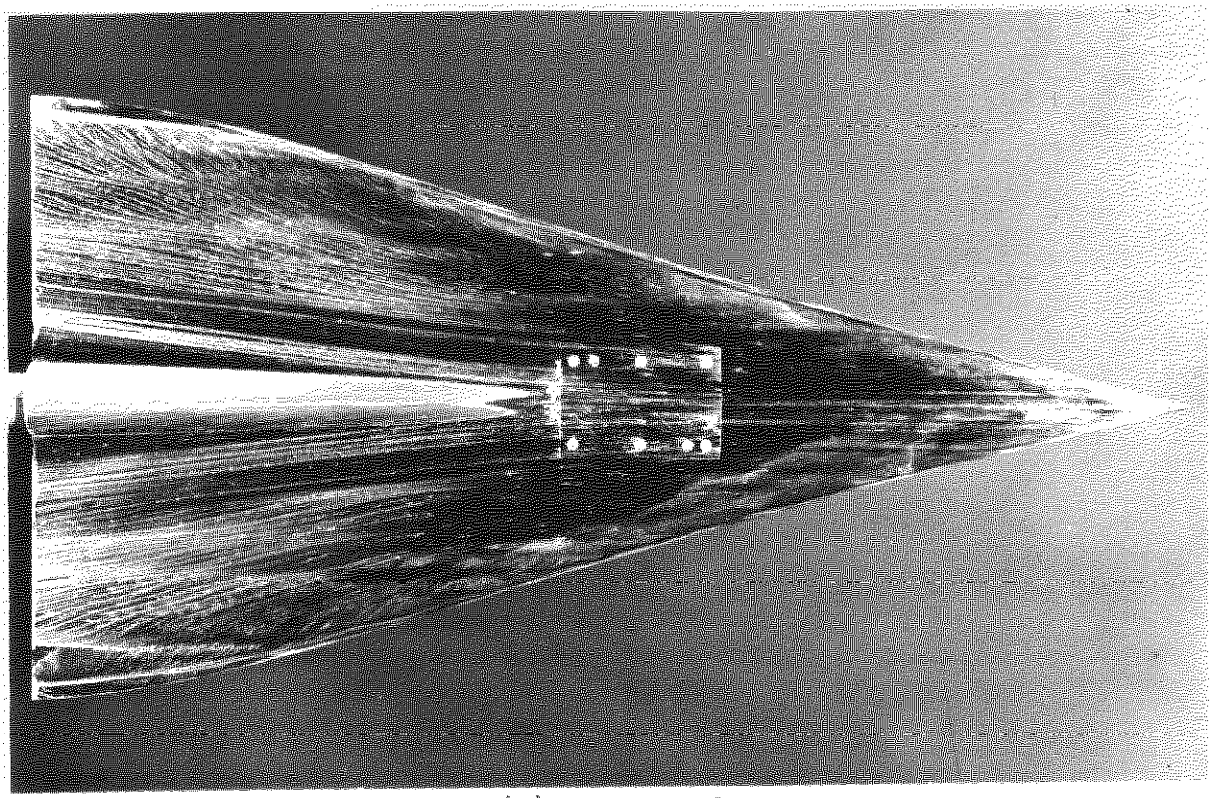

(a) $\alpha = 7.3°$

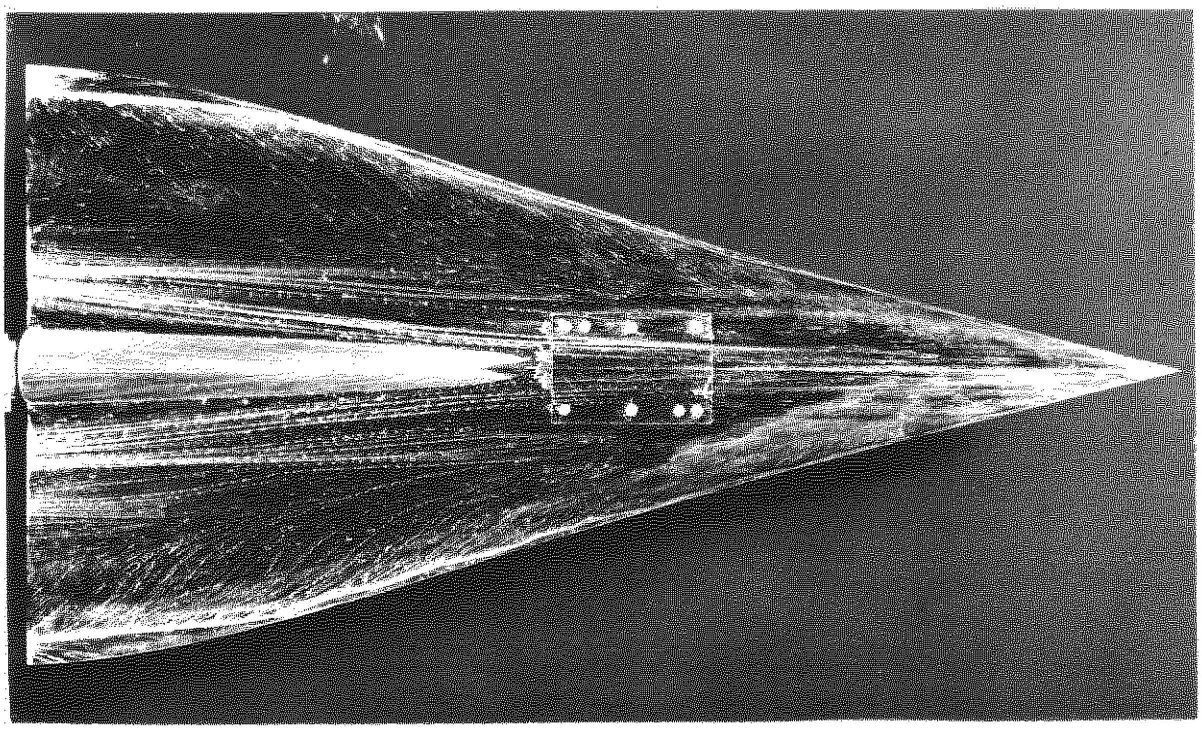

(b) $\alpha = 8.3°$

Fig.27 Wing 10. Oil flow photographs, M = 1·4

A.R.C. C.P. No. 1006
August 1967

533.693.3 :
533.6.011.3 :
533.6.013.13 :
533.6.013.152 :
533.6.013.12 :
533.6.071

Mabey, D.G.
Ilott, G.P.

THE LONGITUDINAL CHARACTERISTICS OF THREE SLENDER "MILD OGEE" WINGS AT MACH NUMBERS FROM 0.4 TO 2.0

Wind tunnel measurements of lift, pitching moment and drag on one plane and two cambered wings of "mild ogee" planform (p = 8/15) are reported. These measurements are supplemented by vapour screen and oil flow observations.

The wings were designed by slender wing theory for attached flow along the leading-edge at particular values of lift and pitching moment. The design and measured attachment conditions agreed fairly well. The non-linear lift developed could be related with the type of vortex development above the attachment incidence.

A.R.C. C.P. No. 1006
August 1967

533.693.3 :
533.6.011.3 :
533.6.013.13 :
533.6.013.152 :
533.6.013.12 :
533.6.071

Mabey, D.G.
Ilott, G.P.

THE LONGITUDINAL CHARACTERISTICS OF THREE SLENDER "MILD OGEE" WINGS AT MACH NUMBERS FROM 0.4 TO 2.0

Wind tunnel measurements of lift, pitching moment and drag on one plane and two cambered wings of "mild ogee" planform (p = 8/15) are reported. These measurements are supplemented by vapour screen and oil flow observations.

The wings were designed by slender wing theory for attached flow along the leading-edge at particular values of lift and pitching moment. The design and measured attachment conditions agreed fairly well. The non-linear lift developed could be related with the type of vortex development above the attachment incidence.

A.R.C. C.P. No. 1006
August 1967

533.693.3 :
533.6.011.3 :
533.6.013.13 :
533.6.013.152 :
533.6.013.12 :
533.6.071

Mabey, D.G.
Ilott, G.P.

THE LONGITUDINAL CHARACTERISTICS OF THREE SLENDER "MILD OGEE" WINGS AT MACH NUMBERS FROM 0.4 TO 2.0

Wind tunnel measurements of lift, pitching moment and drag on one plane and two cambered wings of "mild ogee" planform (p = 8/15) are reported. These measurements are supplemented by vapour screen and oil flow observations.

The wings were designed by slender wing theory for attached flow along the leading-edge at particular values of lift and pitching moment. The design and measured attachment conditions agreed fairly well. The non-linear lift developed could be related with the type of vortex development above the attachment incidence.

DETACHABLE ABSTRACT CARDS

C.P. No. 1006

Published by
HER MAJESTY'S STATIONERY OFFICE

To be purchased from
49 High Holborn, London W C 1
423 Oxford Street, London W 1
13A Castle Street, Edinburgh 2
109 St Mary Street, Cardiff
Brazennose Street, Manchester 2
50 Fairfax Street, Bristol 1
258-259 Broad Street, Birmingham 1
7-11 Linenhall Street, Belfast 2
or through any bookseller

C.P. No. 1006

S.O. CODE No. 23-9018-6